

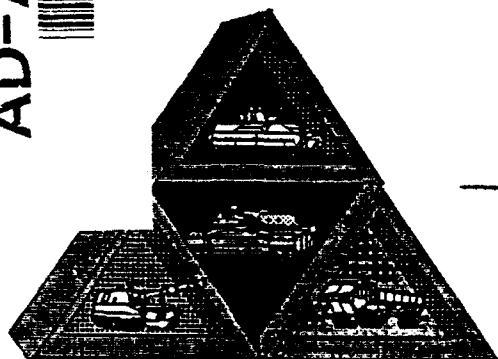
2

AD-A265 888



TARDEC

Technical Report



No. 13591

MI, IPMI and MIAI
(through November 1990) Abrams Tank Lifting
Provisions: Nonlinear Finite Element
Analysis of Front Lifting Eye

93-13563



Original contains color
plates. All DTIC reproductions
will be in black and
white.

DTIC
ELECTE
JUN 16 1993
S B D

93 6 10 25 4 By

Farzad Rostam-Abadi (AMSTA-JSK)
Milton Chaika (AMSTA-RYC)
Stephen Lambrecht (AMSTA-RYC)
Raju Namburu (AHPCRC/CSC)

APPROVED FOR PUBLIC RELEASE:
DISTRIBUTION IS UNLIMITED



U.S. Army Tank-Automotive Command
Research, Development, and Engineering Center
Warren, Michigan 48397-5000

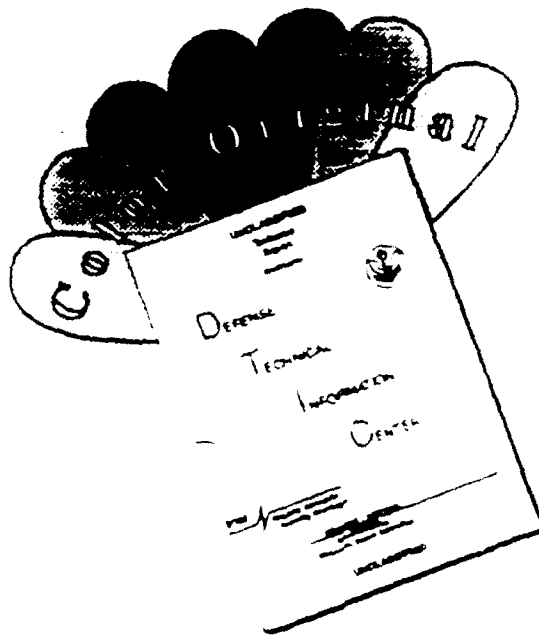
NOTICES

This report is not to be construed as an official Department of the Army position.

Mention of any trade names or manufacturers in this report shall not be construed as an official endorsement or approval of such products or companies by the U.S. Government.

Destroy this report when it is no longer needed. Do not return it to the originator.

DISCLAIMER NOTICE



THIS DOCUMENT IS BEST QUALITY AVAILABLE. THE COPY FURNISHED TO DTIC CONTAINED A SIGNIFICANT NUMBER OF COLOR PAGES WHICH DO NOT REPRODUCE LEGIBLY ON BLACK AND WHITE MICROFICHE.

REPORT DOCUMENTATION PAGE			Form Approved OMB No. 0704-0188	
<small>Public reporting burden for this collection of information is estimated to average 1 hour per response, including the time for reviewing instructions, searching existing data sources, gathering and maintaining the data needed, and completing and reviewing the collection of information. Send comments regarding this burden estimate or any other aspect of this collection of information, including suggestions for reducing this burden, to Washington Headquarters Services, Directorate for Information Operations and Reports, 1215 Jefferson Davis Highway, Suite 1204, Arlington, VA 22202-4302, and to the Office of Management and Budget, Paperwork Reduction Project (0704-0188), Washington, DC 20503</small>				
1. AGENCY USE ONLY (Leave blank)	2. REPORT DATE April 29, 1993	3. REPORT TYPE AND DATES COVERED Final - Nov 92-Mar 93		
4. TITLE AND SUBTITLE M1, IPM1 and M1A1 (through November 1990) Abrams Tank Lifting Provisions: Nonlinear Finite Element Analysis of Front Lifting Eye		5. FUNDING NUMBERS		
6. AUTHOR(S) Stephen Lambrecht, Raju Namburu, Milton Chaika, Farzad Rostam-Abadi				
7. PERFORMING ORGANIZATION NAME(S) AND ADDRESS(ES) US Army Tank-Automotive Command AMSTA-RYC Warren, MI 48397-5000		8. PERFORMING ORGANIZATION REPORT NUMBER 13591		
9. SPONSORING/MONITORING AGENCY NAME(S) AND ADDRESS(ES)		10. SPONSORING/MONITORING AGENCY REPORT NUMBER		
11. SUPPLEMENTARY NOTES				
12a. DISTRIBUTION/AVAILABILITY STATEMENT Approved for Public Release: Distribution Unlimited		12b. DISTRIBUTION CODE		
13. ABSTRACT (Maximum 200 words) <p>The Army is planning to upgrade the existing Main Battle Tank. Concern was expressed whether the current lifting configuration was strong enough to support the additional load of this upgrade. A non-linear finite element analysis of four different configurations was done to determine whether the front lifting eye was strong enough. The analysis indicates that with a spreader bar incorporated in the lifting harness, the eye is strong enough. Without such a spreader bar, a detailed comparison between competing strengthening configurations was made. Additional welds were as strong as full penetration welds. The recommendation was to strengthen the lifting eye by using the additional welds proposed by the Abrams Project Managers' Office.</p>				
14. SUBJECT TERMS Finite Element Analysis Lifting Eye M1-Tank			15. NUMBER OF PAGES 59	
			16. PRICE CODE	
17. SECURITY CLASSIFICATION OF REPORT Unclassified	18. SECURITY CLASSIFICATION OF THIS PAGE Unclassified	19. SECURITY CLASSIFICATION OF ABSTRACT Unclassified	20. LIMITATION OF ABSTRACT	

PREFACE

This report was prepared by personnel from AMSTA-JSK, AMSTA-RYC and AHPCRC/CSC of the U S Army Tank-Automotive Research, Development and Engineering Center (TARDEC) for the Engineering office of the Abrams Project Management Office, Warren, Michigan. The authors wish to acknowledge suggestions provided by Mr. G. Vander Waerden and Mr. T. Manuszak of PM, ABRAMS, Mr. M. Rzyzi of PM, Survivability Systems and General Dynamics Land Systems division engineers. Special thanks are due to Mr. Roberto Garcia of AMSTA-RYC of the U.S. Army TARDEC, Warren, Michigan. The first author would also like to acknowledge Mr. Samuel Goodman (AMSTA-JSK) and Dr. James Thompson (AMSTA-JS) for their helpful suggestions.

Accession For	
NTIS	<input checked="" type="checkbox"/>
DTIC TAB	<input type="checkbox"/>
Unannounced	<input type="checkbox"/>
Justification	
By	
Distribution	
Availability Codes	
Avail and/or	
Dist	Special
A-1	

TABLE OF CONTENTS

PREFACE	2
1.0. INTRODUCTION	7
2.0. OBJECTIVE	7
3.0. CONCLUSIONS	11
4.0. RECOMMENDATIONS	11
5.0. DISCUSSION	12
5.1. <u>INTRODUCTION TO THE FINITE ELEMENT METHOD</u>	12
5.2. <u>MODELING PHILOSOPHY</u>	13
5.3. <u>COMPUTER SOFTWARE AND HARDWARE</u>	14
5.3.1. PATRAN	14
5.3.2. ABAQUS	14
5.4. <u>GEOMETRY OF THE MODELS</u>	14
5.4.1. MATERIALS	16
5.4.2. BOUNDARY CONDITIONS	17
5.4.3. EXISTING LIFTING EYE CONFIGURATION	17
5.4.4. FULL-PENETRATION CONFIGURATION	20
5.4.5. MODIFIED DESIGN ONE	20
5.4.6. MODIFIED DESIGN TWO	20
5.5. <u>DISCUSSION OF RESULTS</u>	20
5.5.1. ASSUMPTIONS	25
5.5.2. EXISTING LIFTING EYE CONFIGURATION	25
5.5.3. FULL-PENETRATION	30
5.5.4. MODIFIED DESIGN ONE	35
5.5.5. MODIFIED DESIGN TWO	35
6.0. REFERENCES	41
APPENDIX A: ADDITIONAL STRESS PLOTS FOR THE EXISTING FRONT LIFTING EYE CONFIGURATION	A-1
APPENDIX B: ADDITIONAL STRESS PLOTS FOR THE FULL-PENETRATION WELD CONFIGURATION	B-1
APPENDIX C: ADDITIONAL STRESS PLOTS FOR THE MODIFIED DESIGN ONE CONFIGURATION	C-1
APPENDIX D: ADDITIONAL STRESS PLOTS FOR THE MODIFIED DESIGN TWO CONFIGURATION	D-1
DISTRIBUTION LIST	Dist-1

LIST OF TABLES

5-1.	RHA Material Properties	16
5-2.	AX-90 Weld Material Properties	16
5-3.	Front Lifting Eye Loads	17
5-4.	Results for Existing Configuration	25
5-5.	Results for Full-Penetration Configuration	30
5-6.	Results for Modified Design One	35
5-7.	Results for Modified Design Two	38

LIST OF FIGURES

Fig. 1-1	Abrams with front lifting eye configuration	8
Fig. 1-2	Abrams lifting provision: Without spreader bar	9
Fig. 1-3	Spreader bar	10
Fig. 5-1	Two types of pressure loadings on front lifting eye	15
Fig. 5-2	Lifting eye with clevis pin	18
Fig. 5-3	Constraints or boundary conditions	19
Fig. 5-4	Existing front lifting eye configuration	21
Fig. 5-5	Full-penetration configuration	22
Fig. 5-6	Modified design one configuration	23
Fig. 5-7	Modified design two configuration	24
Fig. 5-8	Existing configuration: Von Mises stresses at 2.3 times design load with spreader bar	26
Fig. 5-9	Existing configuration: Von Mises stresses at 3.45 times design load with spreader bar	27
Fig. 5-10	Existing configuration: Von Mises stresses at 2.3 times design load without spreader bar	28
Fig. 5-11	Existing configuration: Von Mises stresses at 3.45 times design load without spreader bar	29
Fig. 5-12	Full-penetration weld: Von Mises stresses at 2.3 times design load with spreader bar	31
Fig. 5-13	Full-penetration weld Von Mises stresses at 3.45 times design load with spreader bar	32
Fig. 5-14	Full-penetration weld: Von Mises stresses at 2.3 times design load without spreader bar	33
Fig. 5-15	Full-penetration weld: Von Mises stresses at 3.45 times design load without spreader bar	34
Fig. 5-16	Modified design one: Von Mises stresses at 2.3 times design load without spreader bar	36

Fig. 5-17 Modified design one: Von Mises stresses at 3.45 times design load without spreader bar	37
Fig. 5-18 Modified design two: Von Mises stresses at 2.3 times design load without spreader bar	39
Fig. 5-19 Modified design two: Von Mises stresses at 3.45 times design load without spreader bar	40

1.0. INTRODUCTION

The Army is planning to upgrade existing Abrams main battle tanks to a newer model. The Abrams M1A2 conversion program will provide an Abrams tank with the necessary improvements in lethality, survivability, and fightability required to defeat the threat of the 2000's. This upgrade enhances the capabilities of the older M1-series vehicles but these enhancements add considerable weight to the converted tank. With these additions, the converted M1A2 can weigh up to 70 tons. The Systems Engineering Division of the Abrams Project Manager's Office was concerned whether the current M1 (IPM1 and M1A1) lifting configuration, that portion of the tank by which it is lifted for transportation purposes, would remain strong enough to withstand the additional load. Refer to Fig. 1-1 for other details.

The tank is lifted via a cable harness which is attached at the four corners of the tank. The attachment points on the tank are called lifting eyes. The front lifting eye is a two-piece welded design: an upper portion, the eye, and a lower portion, the base, which is welded to the hull of the tank (Fig. 1-2). There are two types of lifting procedures (see Figs. 1-2 and 1-3) which are given in MIL-STD-209G. One uses a spreader bar (Fig. 1-3) which spreads the load and consequently the stresses on the lifting eye are not as concentrated or severe. The other method has no such spreader bar. Hence, higher stress concentrations are expected to arise when the tank is lifted using no spreader bar. This lifting eye's ability to withstand additional load while the tank was being lifted was the particular concern of the PM Abrams, Systems Engineering Division. This report discusses a detailed three-dimensional nonlinear finite element stress analysis of the front lifting eye for present and proposed designs. Three-dimensional analyses are computationally intensive, hence the analysis was performed on a high-performance computer (CRAY 2).

2.0. OBJECTIVE

The objective of this project was to determine whether the front lifting eyes of the M1, IPM1 and M1A1 (thru November 1990) Abrams tanks are strong enough to support the weight of the heavier M1A2 tank. As requested by the Systems Engineering Division of PM Abrams, the front lifting eyes were used as objects of the stress analysis. A detailed nonlinear three-dimensional finite element analysis--with appropriate design loads and boundary conditions

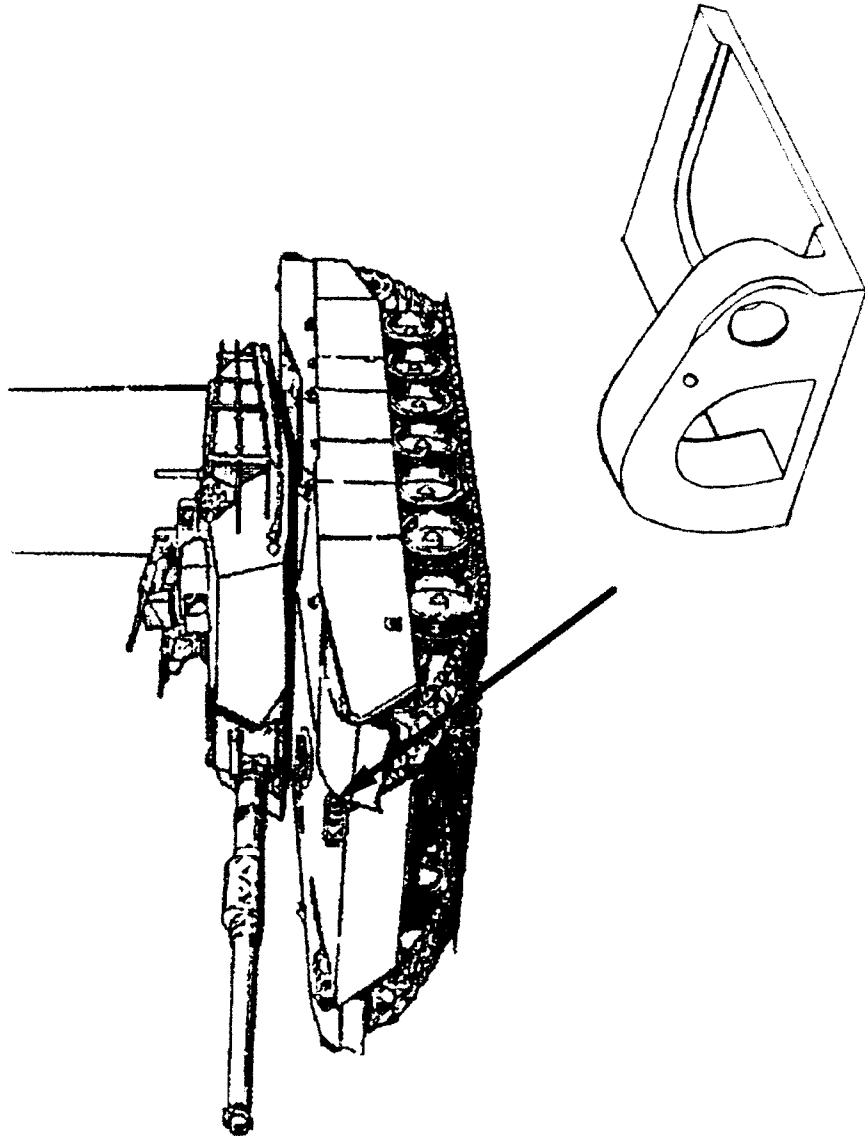


Fig. 1-1 Abrams with front lifting eye configuration

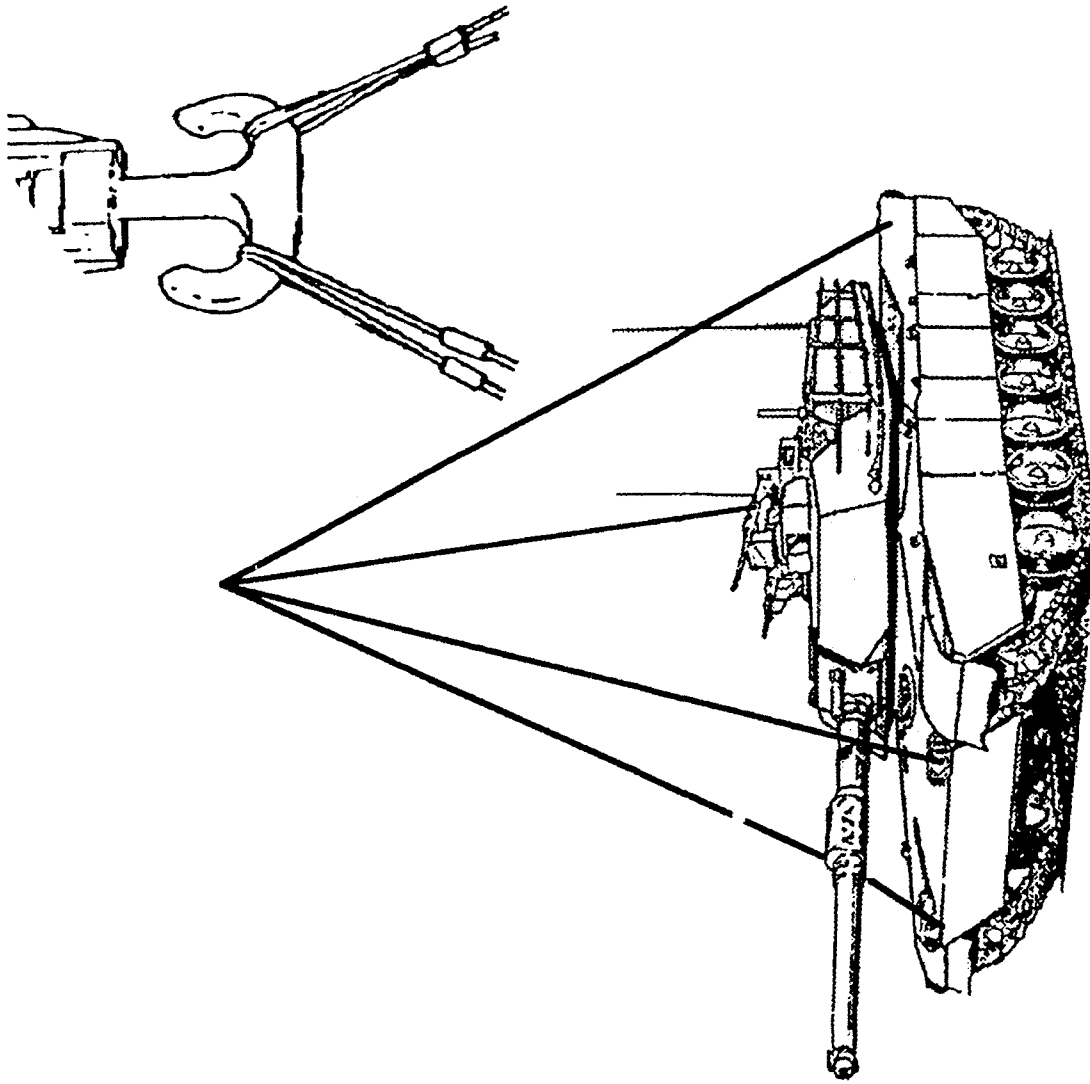


Fig. 1-2 Abrams lifting provision: Without spreader bar

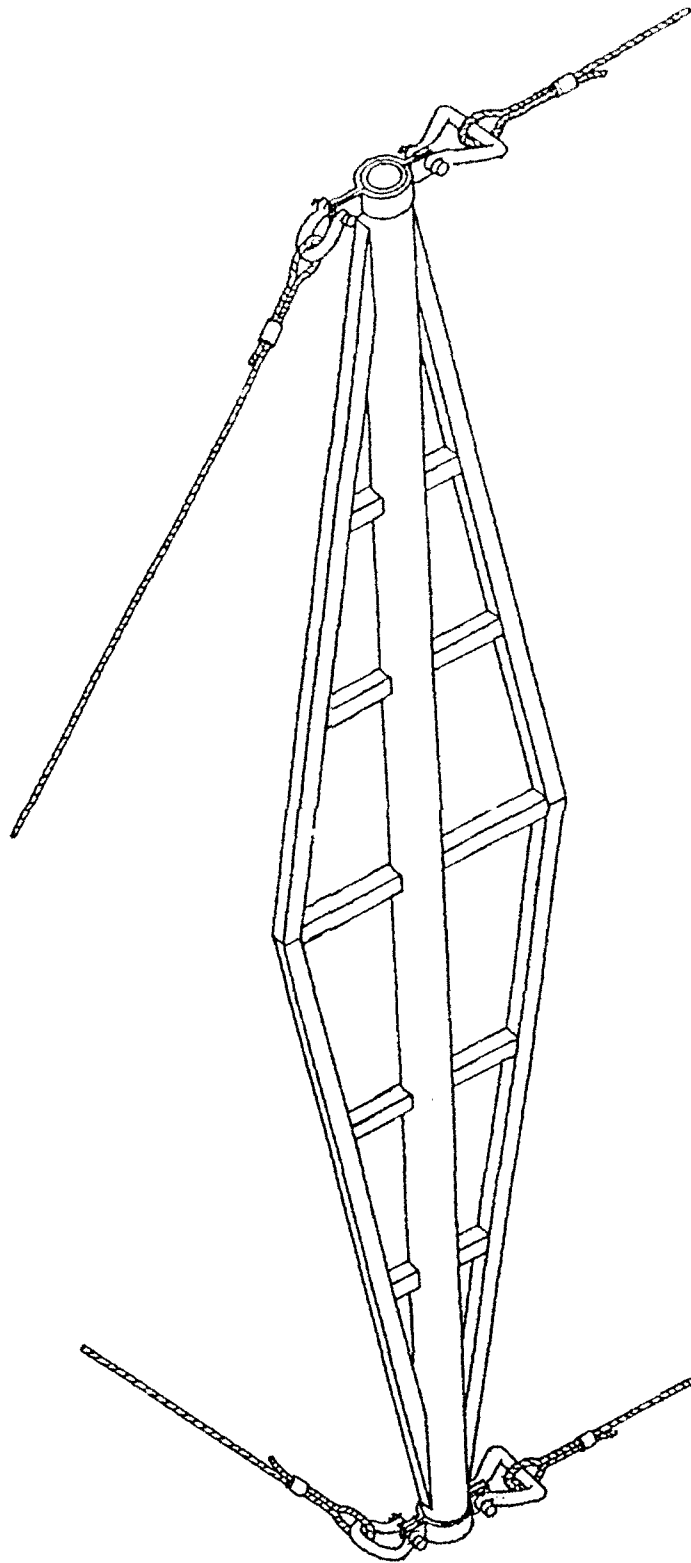


Fig. 1-3 Spreader bar

specified by MIL-STD-209H, AMSTA-T, and General Dynamics Land Systems (GDL S) engineers--was used to analyze the strength of the front lifting eye.

3.0. CONCLUSIONS

The analysis indicates that the front lifting eyes of the M1, IPM1 and M1A1 (thru November 1990) have sufficient strength to support the weight of the M1A2 when a spreader bar is used as part of the lifting harness. When the spreader bar is not incorporated, the lifting eyes have just enough strength to support the vehicle. Specifically, when the lifting harness is used without the spreader bar, the maximum stresses in the lifting eye as obtained by the finite element method are marginally below the criteria for failure as specified by MIL-STD-209H.

To further strengthen the weld, two different configurations were analyzed, namely, full-penetration weld, and an additional weld added to the existing design. Both full-penetration or additional welds will improve the strength of the lifting eye compared to the existing design. It was observed that the differences between maximum stresses in full-penetration analysis and additional weld analysis are marginal (see discussions in section 5.4.1-5.4.5). In addition, the cost involved for adding weld to the existing design is less compared to the full-penetration weld. Due to the above considerations additional welds are recommended. An analysis was also performed to investigate the optimum amount of additional welds and their critical locations.

The analysis follows the recommendations in section 5 of the MIL STD-209-H. Following these recommendations, the results of this report are based on a nonlinear finite element analysis. No fatigue analysis or prototype tests were performed. Also, the lifting eyes were modeled in like-new condition, without cracks or corrosion effects or creep effects.

4.0. RECOMMENDATIONS

It is recommended that the spreader bar always be used when lifting the vehicle. The loads imposed on the lifting eye are about 15 percent lower when the spreader bar is incorporated. It is also recommended that additional welds instead of full-penetration weld be applied to the base of the lifting eye. The strength of the existing weld of the lifting eye can be increased

without incurring much cost by incorporating additional welds, much like the modified models discussed in this report. Since field tests to find the strength of the transportability hardware were to be conducted, it would prove beneficial if the pertinent data were recorded, kept and subsequently compared to those in this study.

5.0. DISCUSSION

5.1. INTRODUCTION TO THE FINITE ELEMENT METHOD

The finite element method is an analysis technique used to solve the differential equations that are the mathematical representative of many complex physical problems. Particularly the finite element method compared to other numerical methods, can solve structural problems that have complex geometry or material characterizations are or that have complex constraints or whose load histories are complex or have any combination of these characteristics. The method can also be used to numerically solve the equations arising from mechanical, thermal-acoustic or fluid mechanic problems or problems that are a combination of these [1].

In solving certain structural problems, the finite element methodology breaks down a continuous complex structure into a finite number of simple discrete regions or elements. Examples of these elements in structural problems are beams, plates, shells, and solids. The elements are then assembled to represent the structure physically. These assembled elements closely model the local deformation of the structure under applied loading and constraints. Thus the model exhibits deformations and stresses or strains of the physical model under the specified loads and constraints. The number of elements used at critical regions is very important to obtain a converged and numerically stable solution, since the finite element method represents continuum problems with discrete elements [2].

The present analysis uses as far as possible, an extremely fine three-dimensional geometric model in order to insure numerical stability and convergence. This fine mesh guarantees that any nuances in stress distribution would be detected and could be distinguished. A nonlinear analysis was performed in order to better model the material changes that the lifting eye underwent under such a large load. The weld's and the rest of the eye were each given material properties obtained from General Dynamics Land Systems and are given in Table 5-1 and 5-2. Due to the accuracy requirements and complexity of the three-dimensional analysis, the

analysis was performed on a CRAY-2 supercomputer. The extent of the weld and its geometry is fully described below as are the various boundary conditions and load cases.

5. 2. MODELING PHILOSOPHY

Engineering intuition and experience indicated that if failure would occur, it would occur at the weld, so the area around the weld was modeled with very fine three-dimensional elements. This would reproduce the deformation history in that area exactly to within possible numerical approximations; similarly, the stress and strain history would be reproduced by this fine model. The problems of numerical stability and convergence were also explored in the modeling and analysis. In contrast, the noncritical areas were modelled using a coarser mesh, since only grosser deformations were of interest.

A modeling methodology used in solving structural problems begins with the failure criteria that the structural component is to satisfy. From these criteria, the area where failure occurs could be identified and the geometric model made to better concentrate on that area. From these criteria, the type of structural analysis is determined, for example, static or dynamic, linear or nonlinear or buckling. Material properties although given may be modified by the failure criteria. Simplifications can be made. A full modeling stratagem thus arises.

The failure criteria given in MIL-STD-209H state that the design limit load will not be less than 2.3 times the static load and the ultimate load will not be less than 1.5 times the design limit load. Using these load factors and the loading configuration given by GDLS and MIL-STD-209H, it was decided that von Mises failure criteria would be used as the conservative method of determining failure. So if a von Mises stress exceeds the yield strength with a 2.3 multiplication factor on the load, or if it exceeds the ultimate strength using a 2.3×1.5 load factor, we would say that the lifting eye failed. This interpretation of the failure criteria in MIL-STD-209H was conveyed in discussions held with engineers from GDLS. The same criteria was employed in the analysis of transportability, tiedown and liftability analysis.

The weld being a critical area, it was decided that the material might not be completely elastic due to large loads, so a nonlinear static analysis with yield strength and ultimate strength given in the appropriate tables was used.

It was felt that a pressure load more realistically modeled the load application. Therefore, the area where the lifting pin contacted the lifting eye was calculated and the load was applied over

that area (Fig. 5-1). Another reason to use pressure loads is to overcome singularities that arise in the numerical methods when point loads or line loads are applied.

Four different finite element models (FEM) were created for this project. The first simulated the actual condition of the front lifting eye of the M1, IPM1 and M1A1 (thru November 1990) tanks. The second simulated the lifting eye with a full-penetration weld. The third and fourth models were proposed modifications to the lifting eyes. For the first two models, both loads, with and without the spreader bar, were analyzed. For the last two models, the analyses simulated the worst-case condition, without the use of a spreader bar.

A nonlinear, static analysis was used for all the models. This was because for the 3.45 load factor, the stresses were going beyond yield, but below the ultimate strength of the material.

5.3. COMPUTER SOFTWARE AND HARDWARE

5.3.1. PATRAN. PATRAN is a pre/post-processing software package developed by PDA Engineering [3]. PATRAN is used to visually create the FEM. PATRAN's post-processor allows the analyst to view the results of the analysis in graphical form. The PATRAN software resides on a Silicon Graphics Personal Iris.

5.3.2. ABAQUS. ABAQUS [4] is a large-scale, general-purpose finite element analysis program capable of analyzing complex structures. The analyst first needs an input file, which in this case was created using PATRAN. The input file defines the shape and material properties of the model, as well as boundary conditions and loads. The program then assembles and solves a system of equations on TARDEC's Cray-2 Supercomputer and outputs the results. ABAQUS was developed by Hibbet, Karlsson, & Sorensen, Inc.

5.4. GEOMETRY OF THE MODELS

The dimensions were taken from Plate drawing No. 12337651 and Eye drawing No. 12337650 of the Abrams tank drawing package. All four models used 3-D solid elements. Thus the models define the actual geometry, material properties, boundary conditions and loading of the actual lifting eye. Also, all models had the welded regions incorporated.

5.4.1. MATERIALS. For this project, two materials were used. M1, IPM1 and M1A1 (thru November 1990) Abrams front lifting eyes are made of MIL-A-12560, which is also

LOAD A = PRESURE WITH SPREADER BAR
LOAD B = PRESURE WITHOUT SPREADER BAR

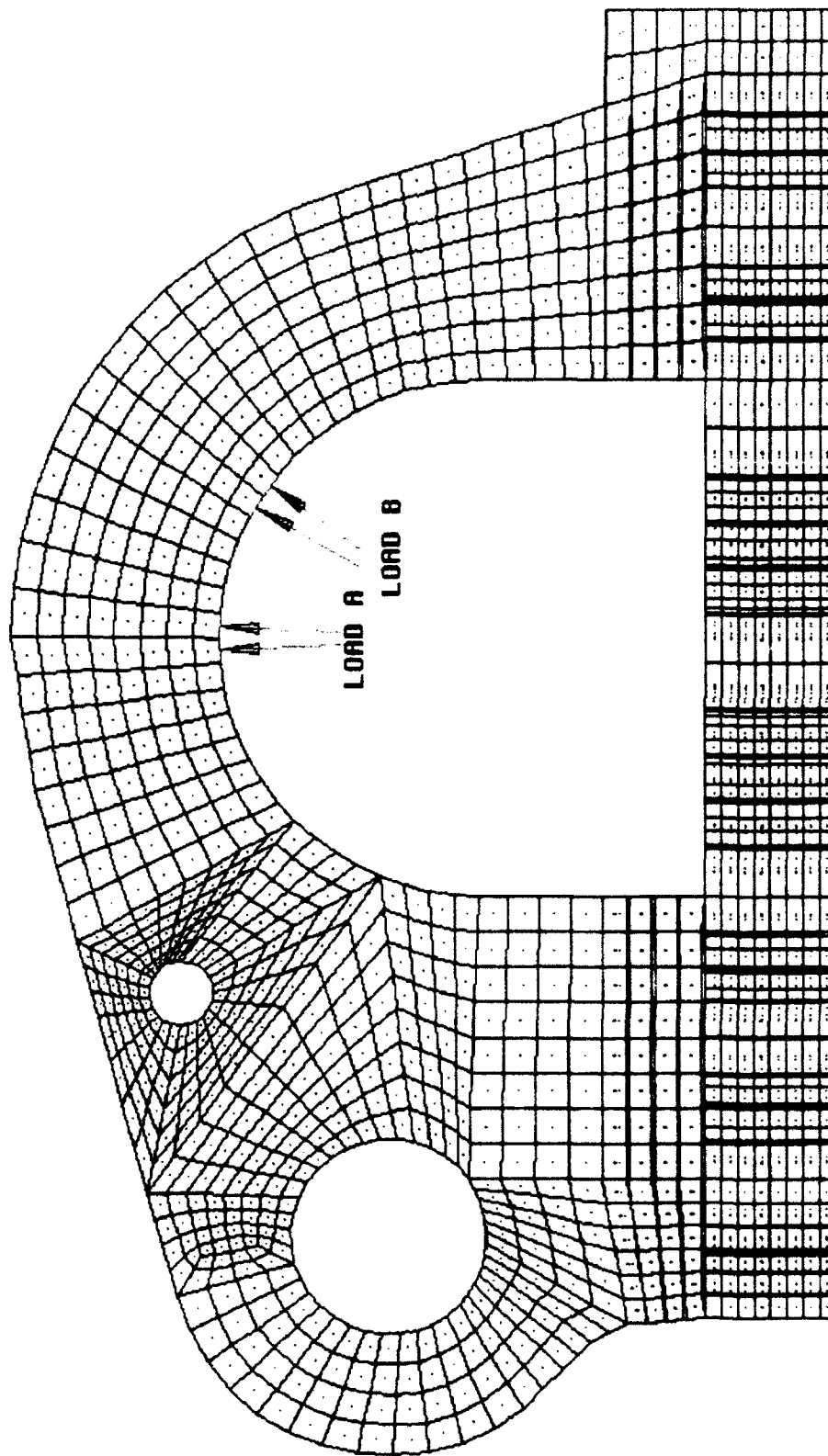


Fig. 5.1 Two types of pressure loadings on front lifting eye

known as rolled homogeneous armor (RHA). The Properties for RHA are listed in TABLE 5-1 below.

Property	Value
Elasticity Constant	29.0×10^6 psi
Poisson's Ratio	0.30
Yield Strength	95 - 153 ksi
Ultimate Strength	115 - 170 ksi

TABLE 5-1. RHA Material Properties

Also, the welded region was modeled for this project. The weld material was an AX-90 wire and the properties are listed in TABLE 5-2 below. When a range is given, the lowest value was used. To be on the conservative side, the lowest value of the range was used in the analysis.

Property	Value
Elasticity Constant	29.0×10^6 psi
Poisson's Ratio	0.30
Yield Strength	90 ksi
Ultimate Strength	110 ksi

TABLE 5-2. AX-90 Weld Material Properties

5.4.2. BOUNDARY CONDITIONS. The loads used in this analysis simulate the vehicle being lifted, with and without the spreader bar. Also, two magnitudes or load factors were used. A design load which was 2.3 times actual, and an ultimate load which was 3.45 times actual were used. The load was applied to the model as a pressure. The area of the contact patch closely resembles the actual contact with a clevis pin. Fig. 5-2 depicts the location of the pressure load on the models. Note that the point of load is different with or without the spreader bar. When looking from the side, the load acts vertically on the lifting eye when the spreader bar is used. When the bar is not used, the load acts at a 41-degree angle from vertical. TABLE 5-3 lists the forces that act on the lifting eye for the varying configurations.

Force with no Load Factor

Direction of Force	With Spreader Bar	Without Spreader Bar
Resultant	36,630 lb	48,870 lb
Longitudinal (X)	0	34,238.6 lb
Vertical (Y)	36,167 lb	36,601 lb
Lateral (Z)	5,806 lb	10,095.3 lb

TABLE 5-3. Front Lifting Eye Loads

All of the models were constrained the same way. The constraints were applied to nodes. The constraints were applied around the edge of the base of the lifting eye models. As can be seen in Fig. 5-3, the front and rear edges of the lifting eye model were constrained from moving in the vertical (Y) and longitudinal (X) directions. The left and right edges of the base were constrained from moving in the vertical (Y) and lateral (Z) directions. This boundary condition closely resembles the actual condition where the lifting eye is welded to the hull of the vehicle.

5.4.3. EXISTING LIFTING EYE CONFIGURATION. This model has the welds and a gap of 0.030" in the exact locations as those of the actual lift eye. In this report the model is called existing1 and existing2. Existing1 uses the 2.3 load factor and no spreader bar, and existing2 uses the 3.45 load factor and no spreader bar. These models have 13,160 solid elements and 16,007 nodes. The suffix B on the names means that the analysis was run with spreader bar loads. In Fig. 5-4 the blue area is the RHA steel and the red area is the weld material.

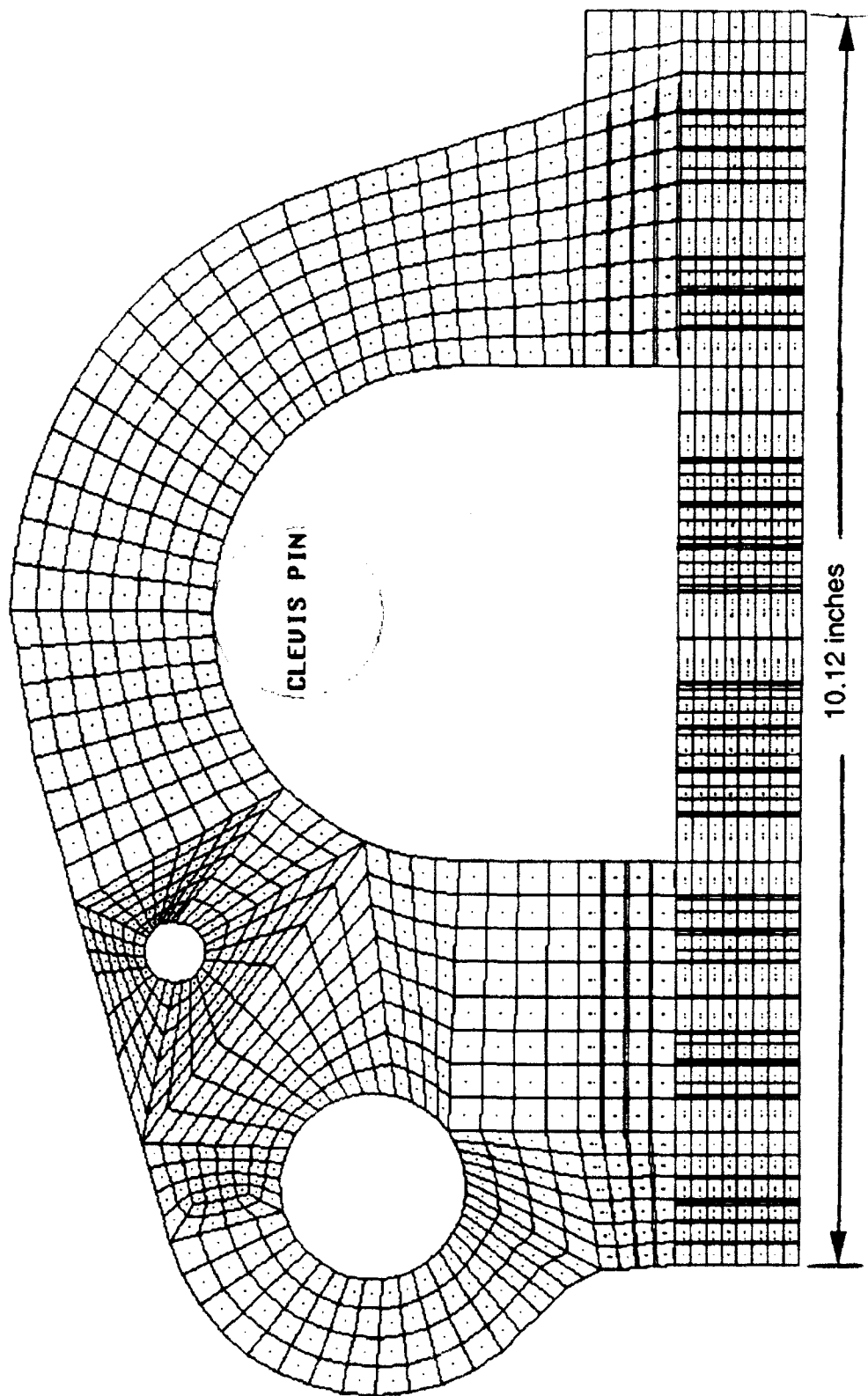


Fig. 5-2 Lifting eye with clevis pin

FRONT LIFTING EYE MODEL

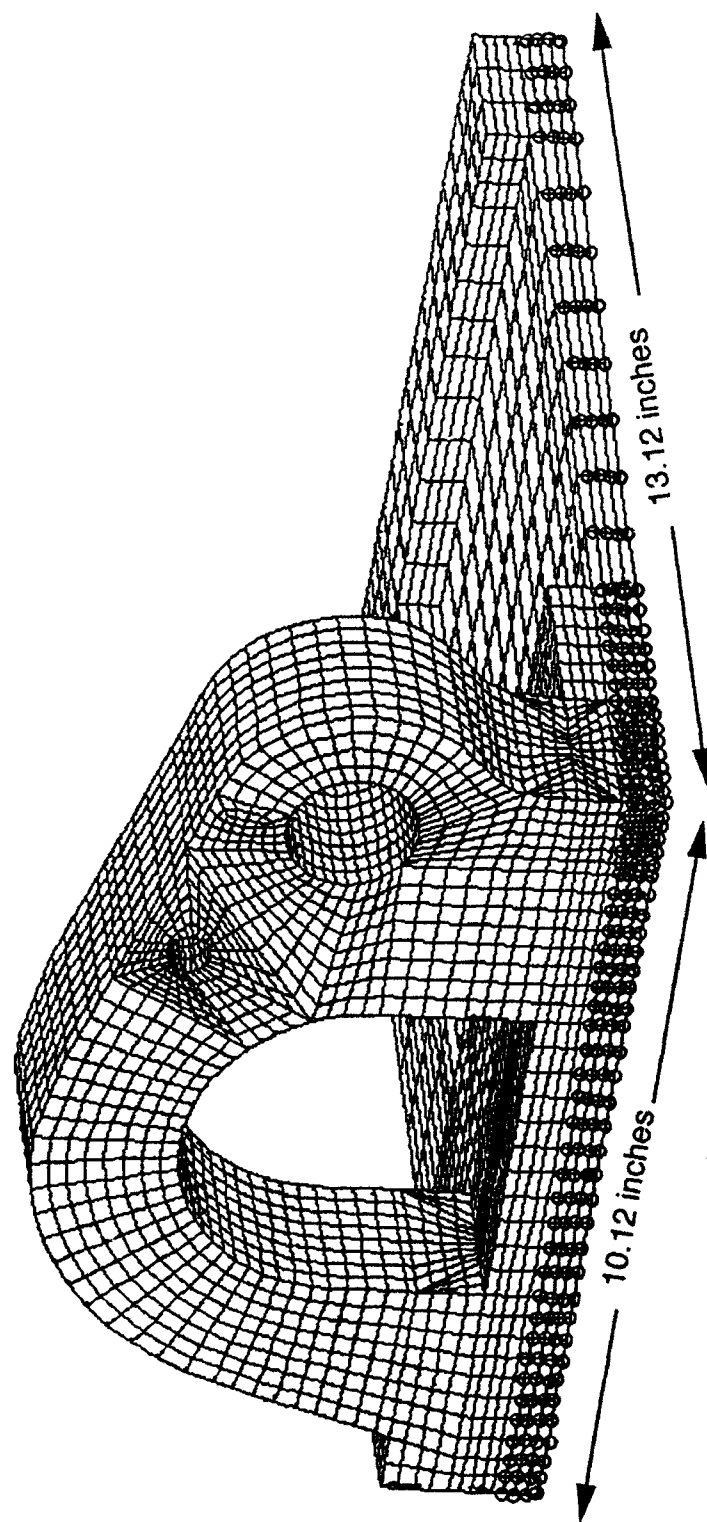


Fig. 5-3 Constraints or boundary conditions

5.4.4. FULL-PENETRATION CONFIGURATION. This model was created to determine the added strength if a full-penetration weld was present. That is, there is no gap in this model. The model is called Fullweld in this report. The suffix of a B means the analysis was run with spreader bar loads. The finite element models for this case have 13,160 solid elements and 15,860 nodes. See Fig.5-5.

5.4.5. MODIFIED DESIGN ONE. It is clearly evident that the full-penetration configuration increases the strength of the lifting eye, but fabrication procedures may cause distortion or material property changes to the lifting eye and/or parent material. Hence, two additional models which minimize fabrication procedures were created to study the strength effects of additional welds versus the existing design and the full-penetration weld design on the lifting eye. The first model was suggested by General Dynamics Land Systems engineers. As can be seen in Fig. 5-6, fillet welds were added around the base of the eye for added strength. This model is named Modone, which is short for Modified Design One. Some portion of the base plate, which is not contributing to the analysis was removed, hence this model has 12,427 solid elements and 14,354 nodes.

5.4.6. MODIFIED DESIGN TWO. This modified design two was similar to the modified design one but had a few less fillet welds at the back of the eye. The basic motivation is to investigate optimum weld area to increase the strength and find the best location of additional welds. See Fig. 5-7. Similar to the above modified design, this model has 12326 solid elements and 14299 nodes.

5.5. DISCUSSION OF RESULTS

After the models were completed in PATRAN, the analysis was run using the Cray-2 Supercomputer. The result files were then translated and post-processing was done using PATRAN. The color stress plots in this report were done using PATRAN. For this project, the von Mises stress criterion, also known as the Maximum Distortion Energy criterion, was used to interpret the results. According to the criterion, a given structural component is safe as long as the maximum value of the distortion energy per unit volume in that material remains smaller than the distortion energy per unit volume required to cause yield in the standard tensile test specimen of the same material. For the 2.3 load factor, the von Mises stress from the analysis was compared to the yield strength of the material. For the 3.45 load factor, the

RED = WELD MATERIAL
BLUE = RHA STEEL

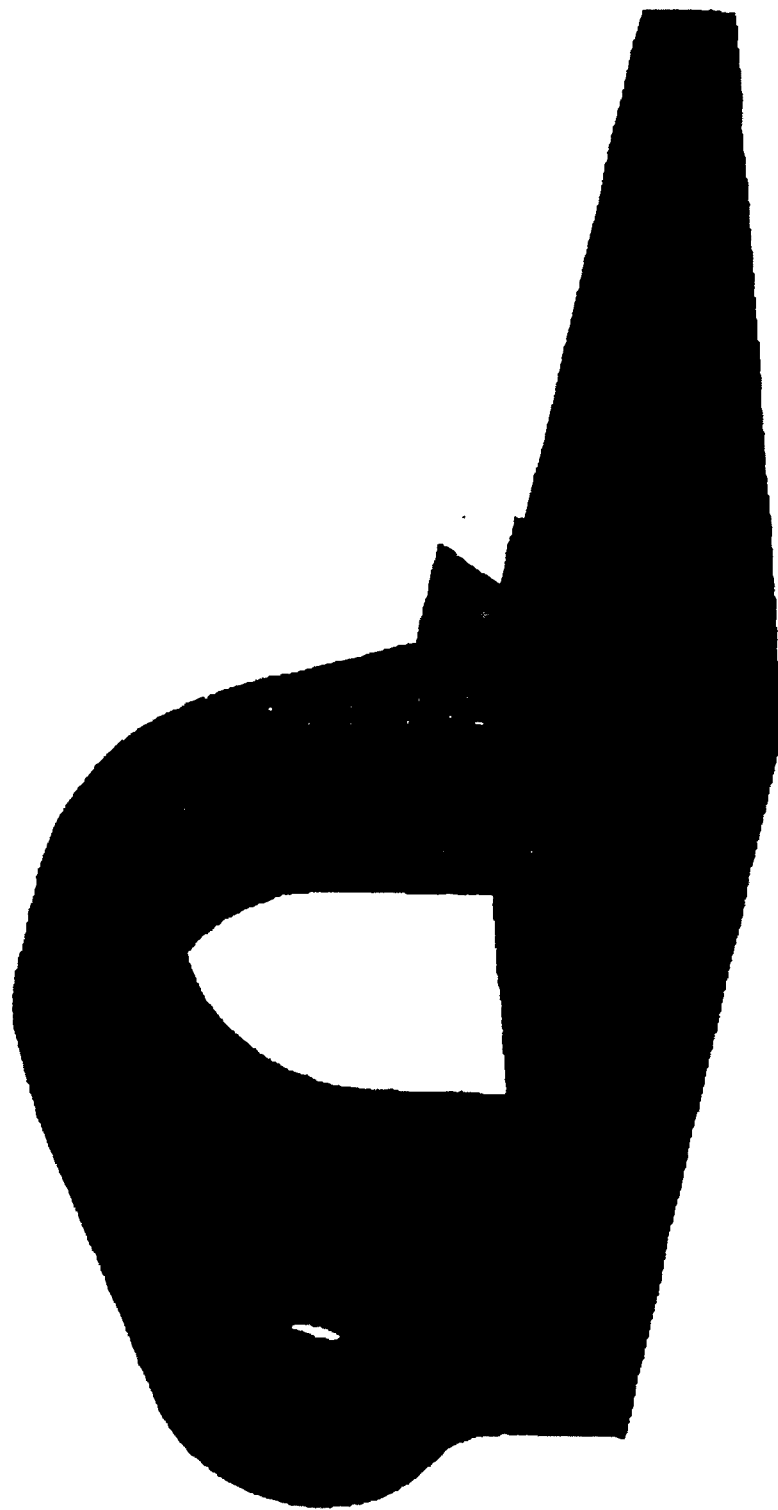


Fig. 5-4 Existing front lifting eye configuration

RED = WELD MATERIAL
BLUE = RHA STEEL



Fig. 5-5 Full-penetration configuration

RED = WELD MATERIAL
BLUE = RHA STEEL



Fig. 5-6 Modified design one configuration

RED = WELD MATERIAL
BLUE = AHA STEEL



Fig. S-7 Modified design two configuration

maximum von Mises stress was compared to the ultimate strength of the material. If the stress was less than the material strength, the part was said to be safe. Von Mises stress takes into account the shear stress effect, as well as the normal stress.

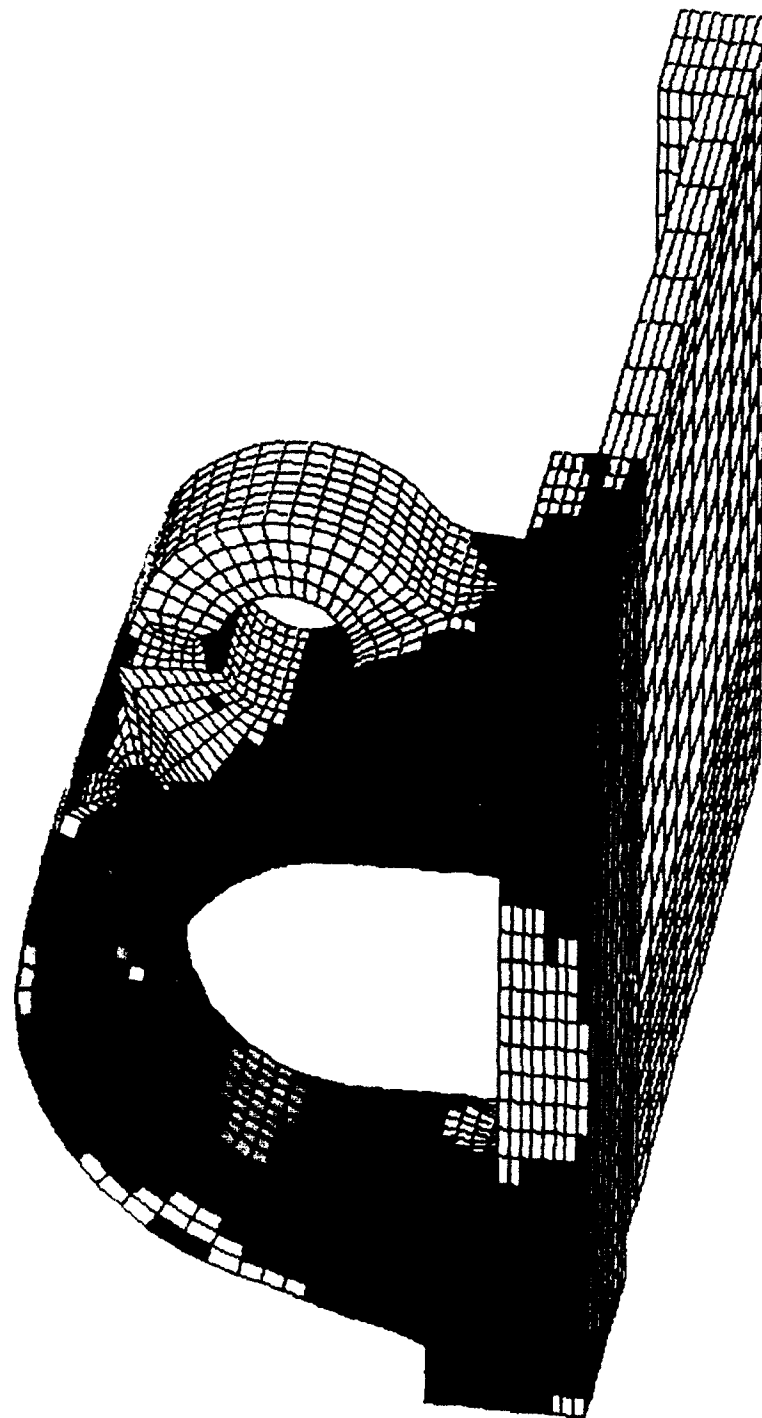
5.5.1. ASSUMPTIONS. Following are the basic assumptions in this analysis: The lifting eyes were modeled in like-new condition, without cracks or corrosion effects or creep effects. No fatigue analysis or prototype tests were performed. Further, the bottom base plate was fixed to the top of the hull of the tank.

5.5.2. EXISTING LIFTING EYE CONFIGURATION. The results of the analysis show that the strength of the current lifting eye on the M1, IPM1 and early M1A1 is marginally lower than the strength required in MIL STD-209H for a 70-ton tank. TABLE 5-4 shows that without the spreader bar the yield stresses in the model exceed the yield strength for the case of 3.45 times the maximum load. TABLE 5-5 also summarizes the results which are shown in Figs. 5-8 to 5-11. The results in Figs. 5-8 to 5-11 show the von Mises stresses in the lifting eye on the outboard side of the vehicle. Note that the yield stresses in five elements on one side and one or two elements on the other exceed the von Mises criterion. Three observations should be made: only the yield criterion is exceeded, not the ultimate strength; No failure occurs in the weld area; the area of yield failure is only one element deep, indicating that much load-carrying capability still remains. The remaining figures that describe the analysis may be found in Appendix A.

File Name	Yield Strength (psi)	Ultimate Strength (psi)	Load Factor	Von Mises Stress (psi)	Location
Existing1B	95,000	115,000	2.3	79,507	in RHA
Existing1B	90,000	110,000	2.3	26,532	in weld
Existing2B	95,000	115,000	3.45	97,082	in RHA
Existing2B	90,000	110,000	3.45	51,809	in weld
Existing1	95,000	115,000	2.3	98,856	in RHA
Existing1	90,000	110,000	2.3	72,505	in weld
Existing2	95,000	115,000	3.45	96,307	in RHA
Existing2	90,000	110,000	3.45	89,915	in weld

TABLE 5-4. Results for Existing Configuration

VON MISES STRESS (PSI)



79507.	
74209.	A
68912.	B
63614.	
58317.	
53020.	E
47722.	F
42425.	
37127.	H
31830.	I
26532.	J
21235.	K
15937.	L
10640.	M
5342.	N

45.0

Fig. 5-8 Existing configuration: Von Mises stresses at 2.3 times design load with spreader bar

VON MISES STRESS (PSI)

97082.
90615.
84147.
77679.
71212.
64744.
58276.
51809.
45341.
38874.
32406.
25938.
19471.
13003.
6535.

67.7

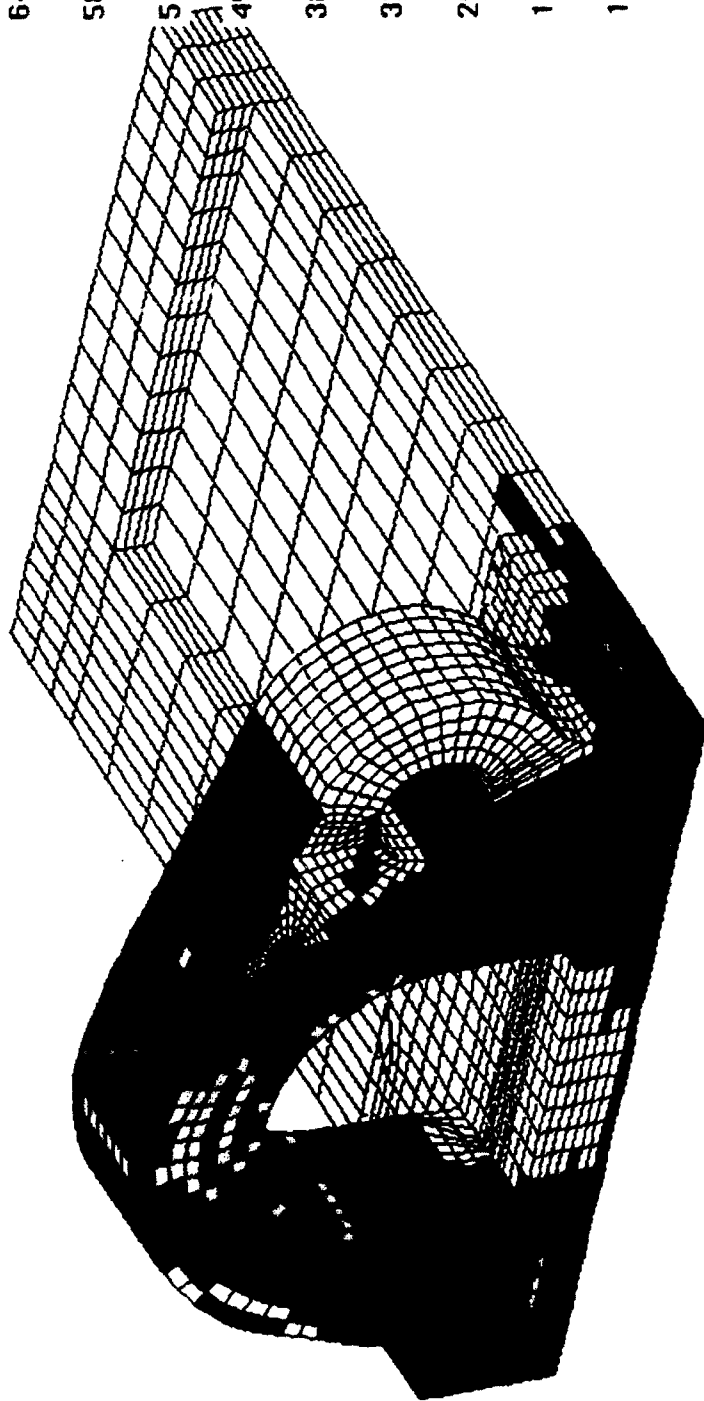


Fig. 5-9 Existing configuration: Von Mises stresses at 3.45 times design load with spreader bar

VON MISES STRESS (PSI)

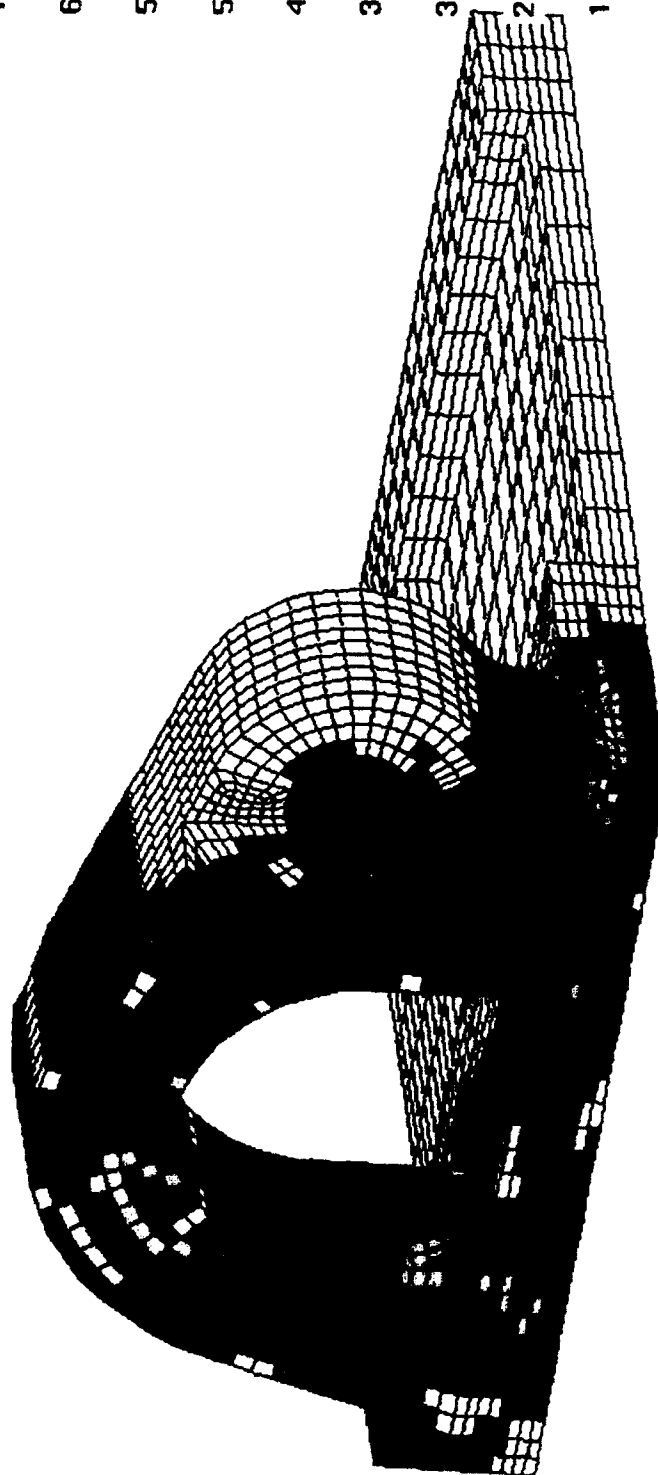
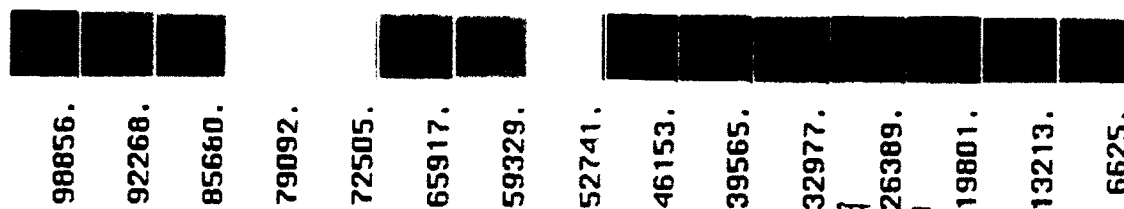
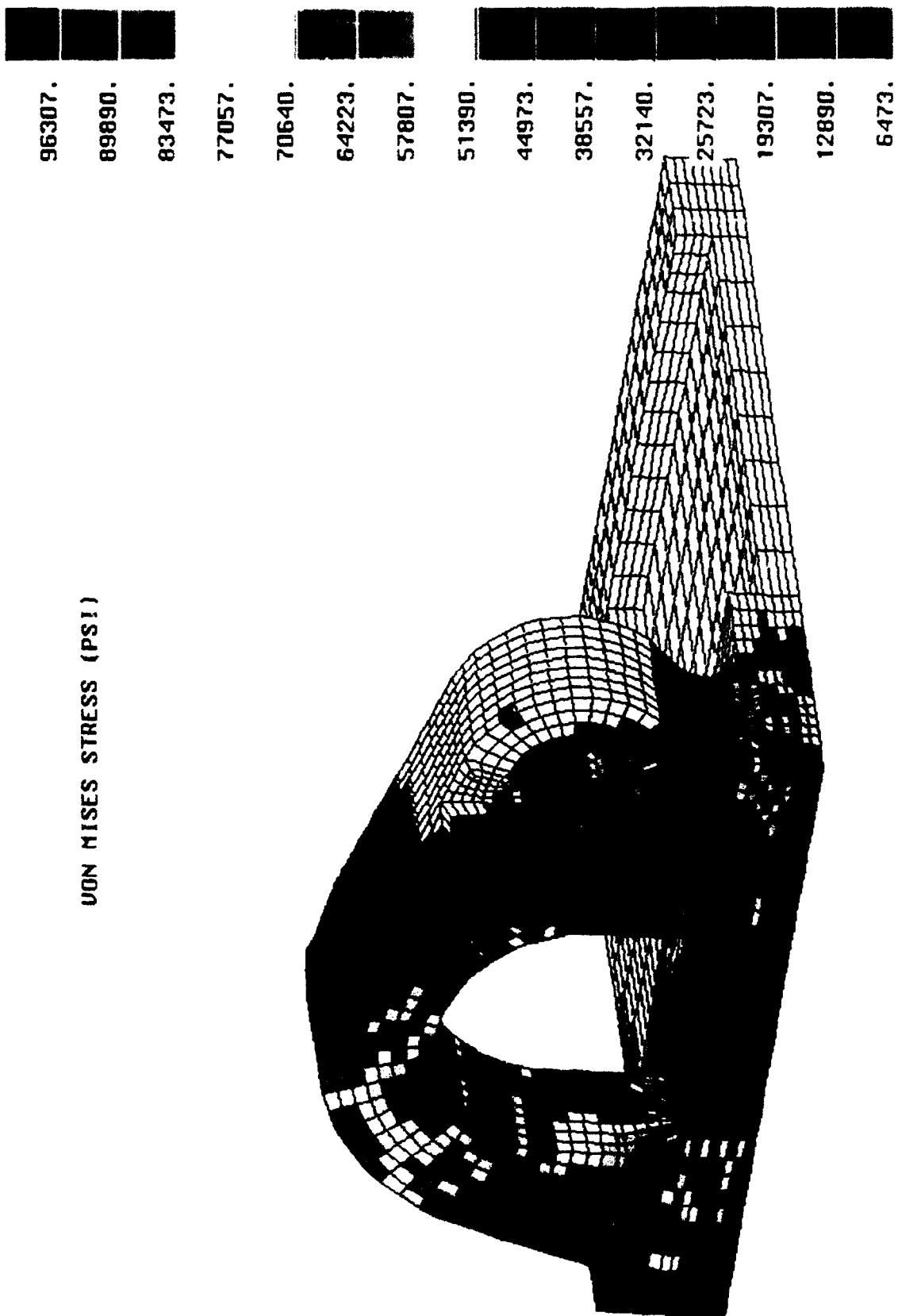


Fig. 5-10 Existing configuration: Von Mises stresses at 2.3 times design load without spreader bar 37.4



56.8

Fig. 5-11 Existing configuration: Von Mises stresses at 3.45 times design load without spreader bar

5.5.3. FULL-PENETRATION. A description of the full-penetration weld may be found in section 5.4.4. Again the lifting configuration with the spreader bar results in stresses that meet the failure criteria of MIL-STD 209H for a 70-ton tank, See Figs 5-12 to 5-15. The summary of these results is in TABLE 5-5 below. The nonlinear static analysis for the load applied without the spreader bar are illustrated in Figs. 5-12 to 5-15. As before, the higher stresses are on the outboard side, Figs 5-12 to 5-15. Throughout the analysis it can be seen that the highest stresses seem to appear where the clevis pin meets the lifting eye. These stresses are highly inaccurate and are probably due to the singularity in the numerical algorithms. The von Mises criterion shows no ultimate failure with a load factor of 2.3×1.5 (3.45) times the actual load, according to MIL STD 209H. The ultimate failure criteria are met in the weld zone. There are two corner elements that have the highest stress within the failure criteria of MIL-STD-209H. In the base there are two areas of high stresses whose maxima are within the criteria. Figs.5-12 to 5-15 show the stresses for the yield criteria in MIL-STD-209H. The yield criteria are met and TABLE 5-5 summarizes the results. The results for the inboard side as well as the rest of the figures are given in Appendix B.

File Name	Yield Strength (psi)	Ultimate Strength (psi)	Load Factor	Von Mises Stress (psi)	Location
Fullweld1B	95,000	115,000	2.3	79,505	in RHA
Fullweld1B	90,000	110,000	2.3	31,892	in weld
Fullweld2B	95,000	115,000	3.45	93,857	in RHA
Fullweld2B	90,000	110,000	3.45	50,089	in weld
Fullweld1	95,000	115,000	2.3	95,172	in RHA
Fullweld1	90,000	110,000	2.3	76,145	in weld
Fullweld2	95,000	115,000	3.45	103,484	in RHA
Fullweld2	90,000	110,000	3.45	96,589	in weld

TABLE 5-5. Results for Full-Penetration Weld

5.5.4. MODIFIED DESIGN ONE. After discussions with the PM Abrams and General Dynamics Land Systems regarding the above existing designs and full-penetration

VON MISES STRESS (PSI)

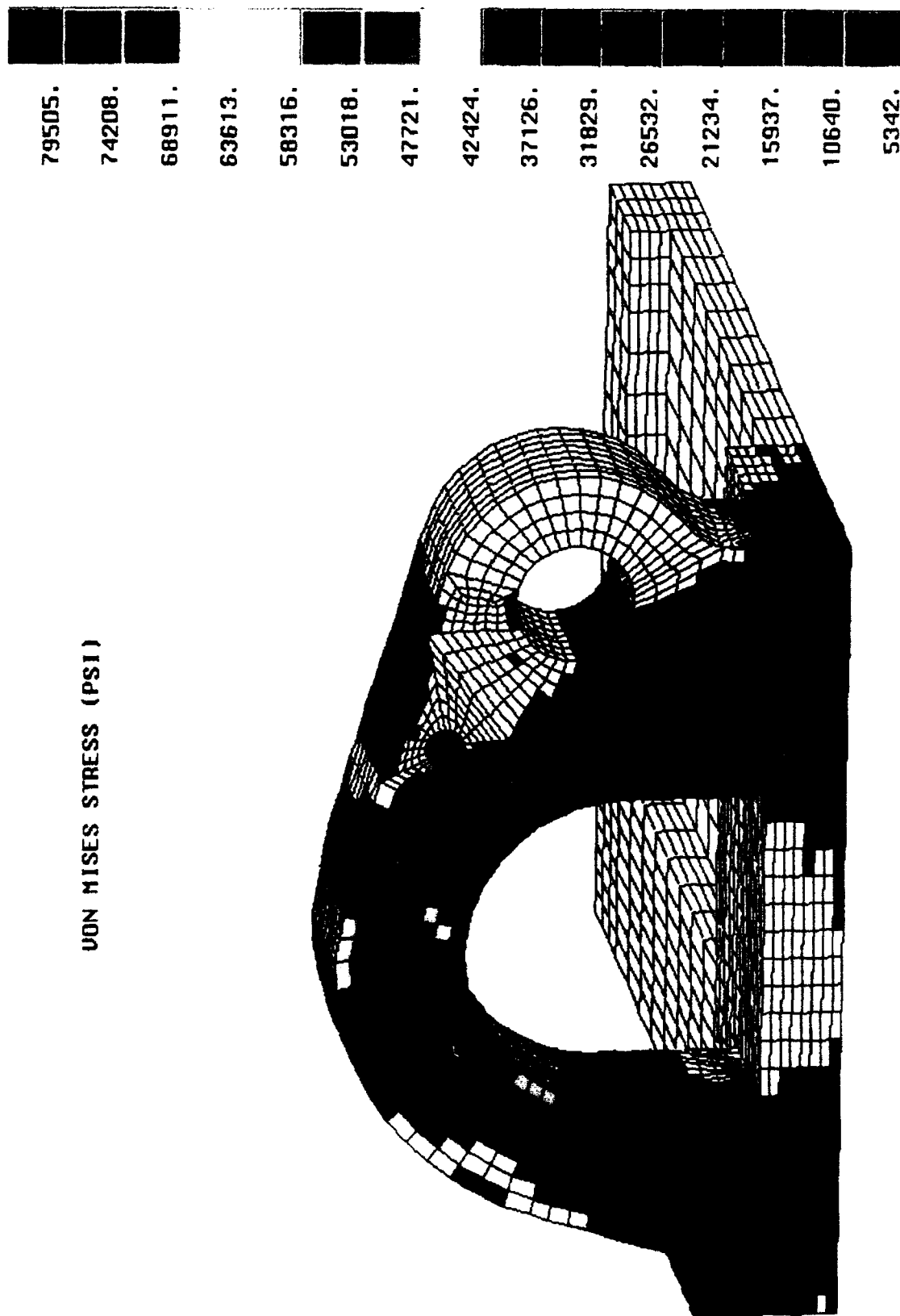


Fig. 5-12 Full-penetration weld: Von Mises stresses at 2.3 times design load with spreader bar 45.0

VON MISES STRESS (PSI)

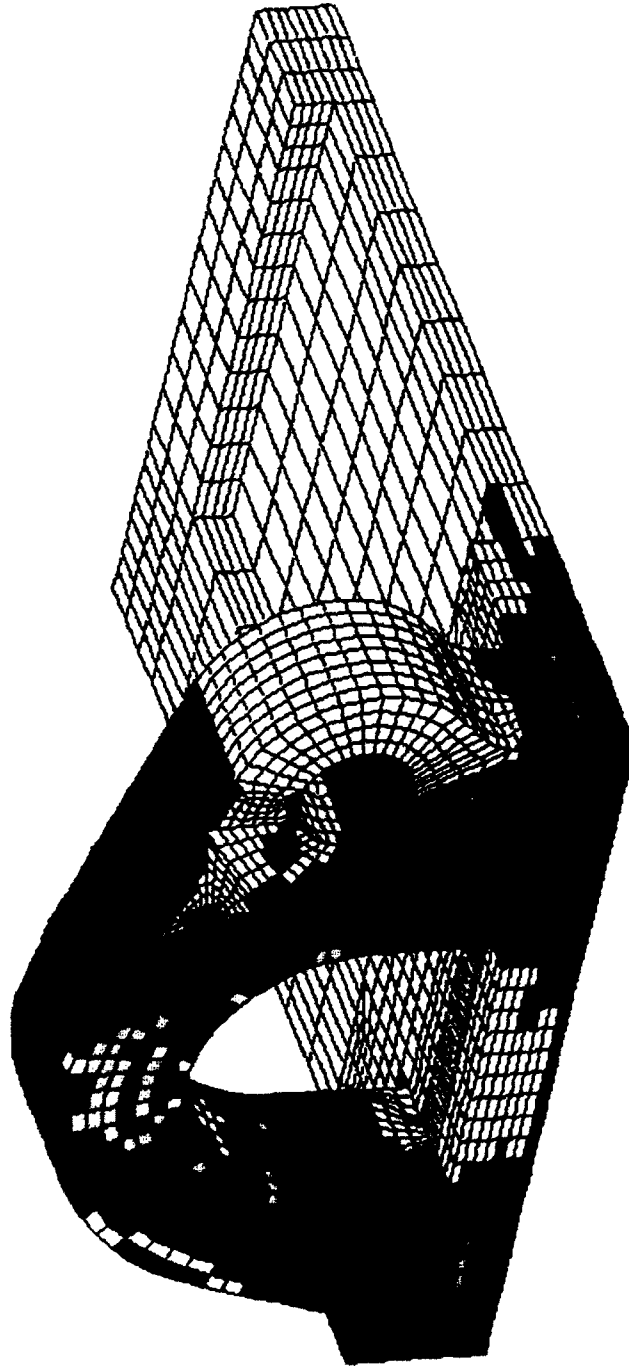
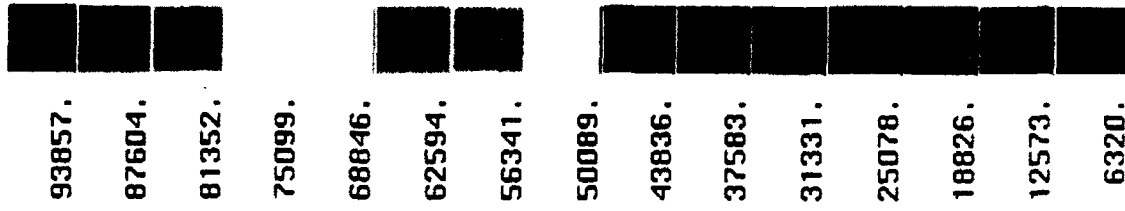


Fig. 5-13 Full-penetration weld Von Mises stresses at 3.45 times design load with spreader bar

67.8

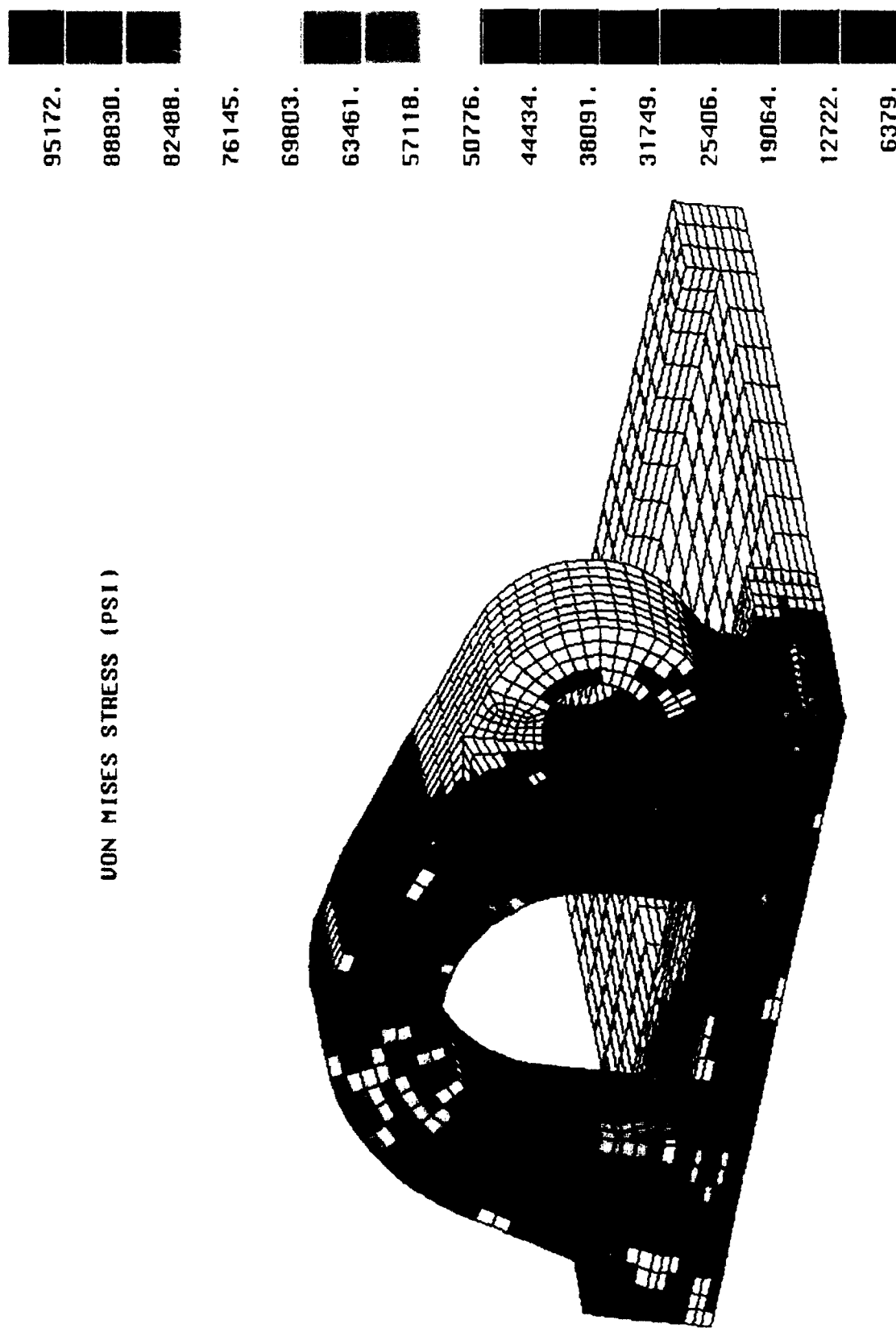


Fig. 5-14 Full-penetration weld: Von Mises stresses at 2.3 times design load without spreader bar

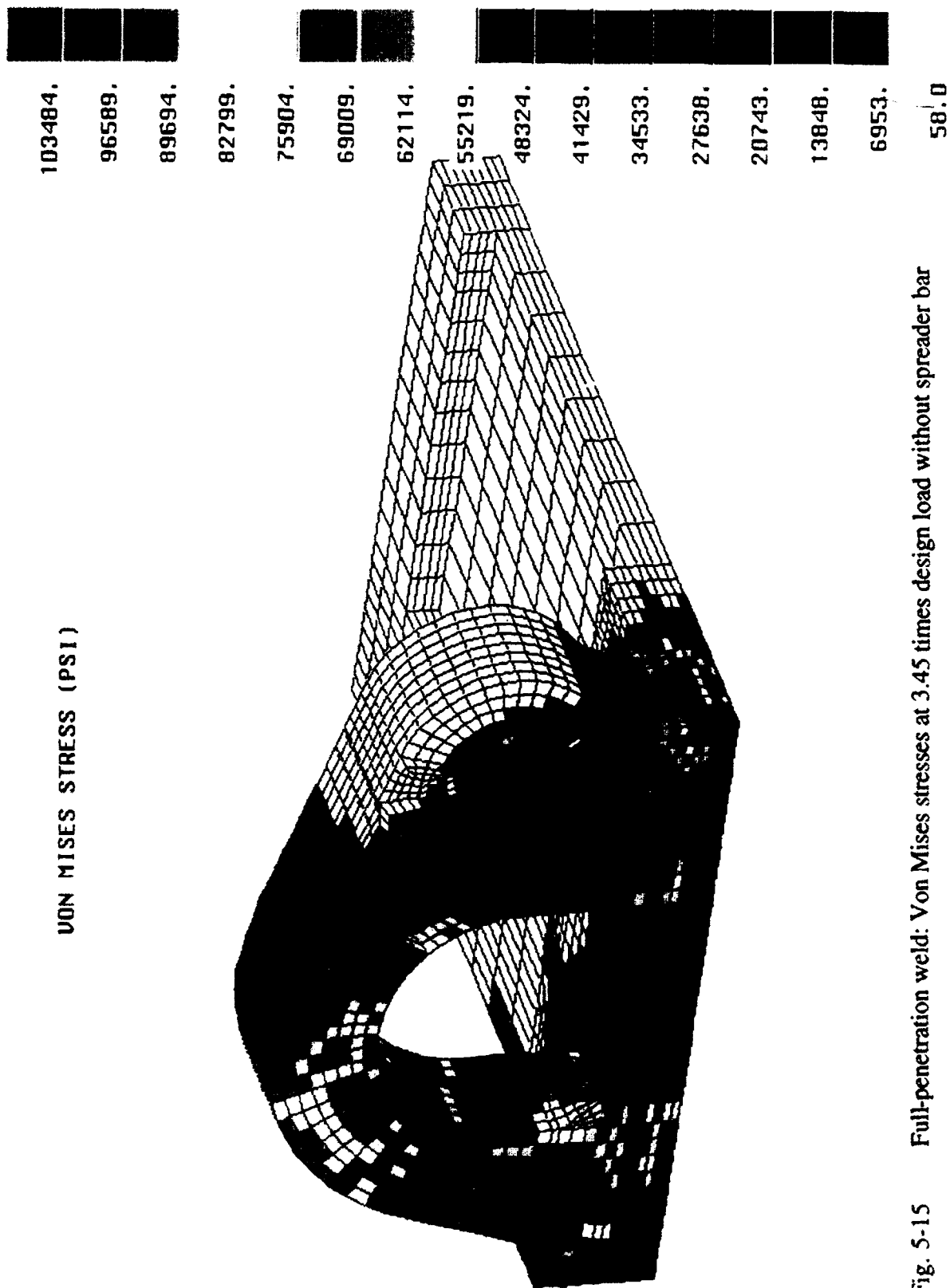


Fig. 5-15 Full-penetration weld: Von Mises stresses at 3.45 times design load without spreader bar

weld analysis, GDLS has provided a design for strengthening the weld. The results for this analysis with no spreader bar are shown in Figs. 5-16, 5-17 and TABLE 5-6. A comparison between this model and the existing design shows that using similar conditions, a decrease occurs in the nonweld area for the yield, but an increase occurs in the model for the ultimate strength criteria. In the weld area, the critical one, there are no real differences in the maxima of the yield or of the ultimate strength criteria. An examination of the weld area for the yield condition shows that in the existing design the high stresses, that is, those above 60,000 psi, are over a larger area and are more concentrated in the corner of the weld. The outboard side of the modified design has the high stresses outside the weld area. The other areas of high stresses are on two elements on the additional weld, that weld that is part of this design modification (refer to Fig. 5-16 to 5-17). This type of distribution is even more pronounced for the failure criteria that use a load factor of 3.45 times the actual load. Again note that in the weld, stresses are higher and cover a larger area on the original model (for comparison see Figs. 5-10 and 5-11 versus Figs. 5-16 and 5-17). To complete the analysis the remaining figures may be found in Appendix C.

File Name	Yield Strength (psi)	Ultimate Strength (psi)	Load Factor	Von Mises Stress (psi)	Location
Modone1	95,000	115,000	2.3	90,935	in RHA
Modone1	90,000	110,000	2.3	72,937	in weld
Modone2	95,000	115,000	3.45	103,295	in RHA
Modone2	90,000	110,000	3.45	96,505	in weld

TABLE 5-6. Results for Modified Design One

5.5.5. MODIFIED DESIGN TWO. The results for this modified eye were very similar to those of the modified design 1 discussed above. As can be seen in the summary TABLE 5-6 and TABLE 5-7, the maximum von Mises stresses in the Modtwo model were all slightly lower than those in the Modone model, except for one. The Modtwo2 result had a maximum von Mises stress of 115,000 psi. This value just passes and is higher than the 103,295 psi maximum von mises stress witnessed in the Modone2 results (see Figs. 5-18 and 5-19). Appendix D contains the rest of the figures for the analysis.

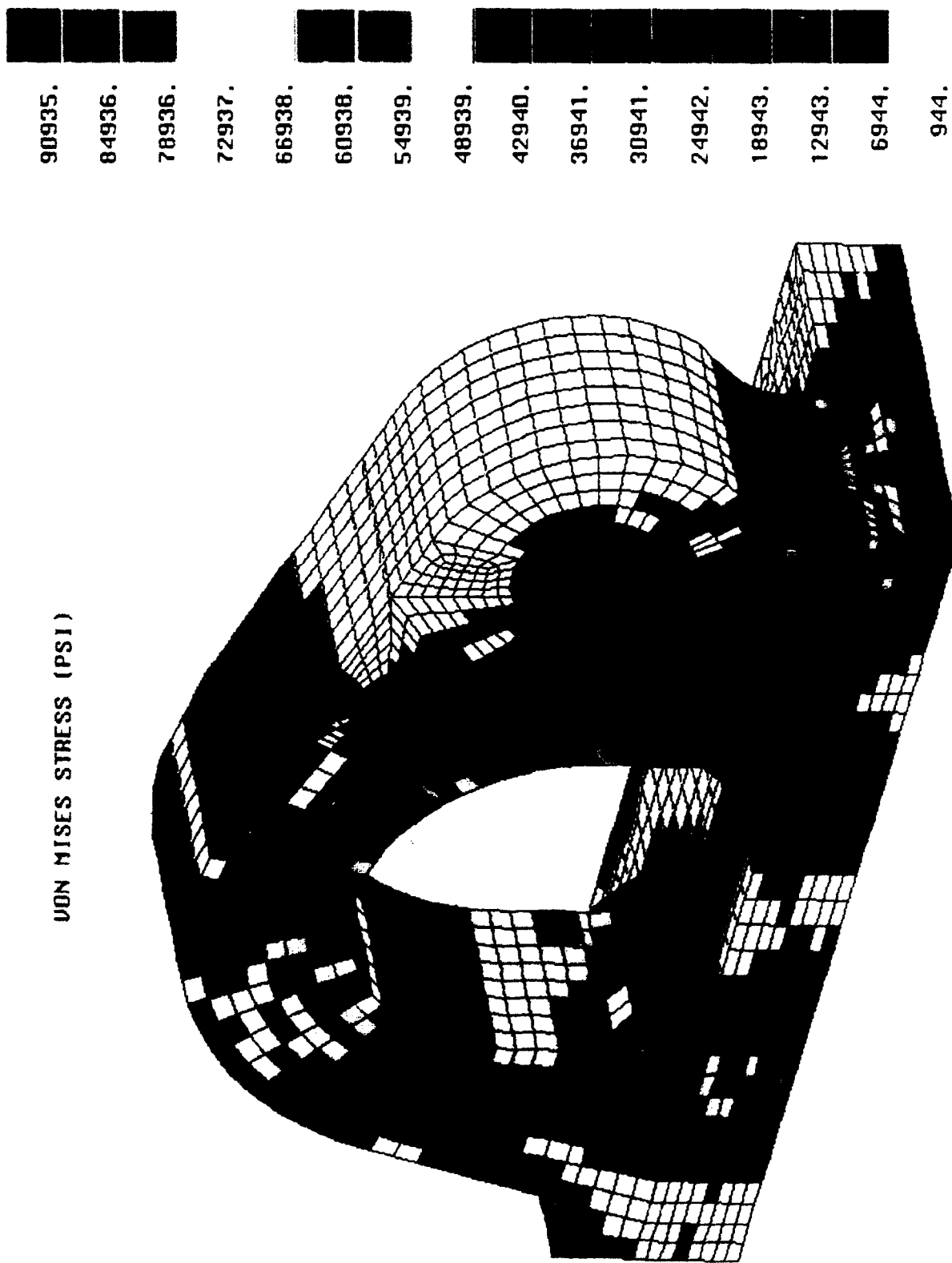


Fig. 5-16 Modified design one: Von Mises stresses at 2.3 times design load without spreader bar

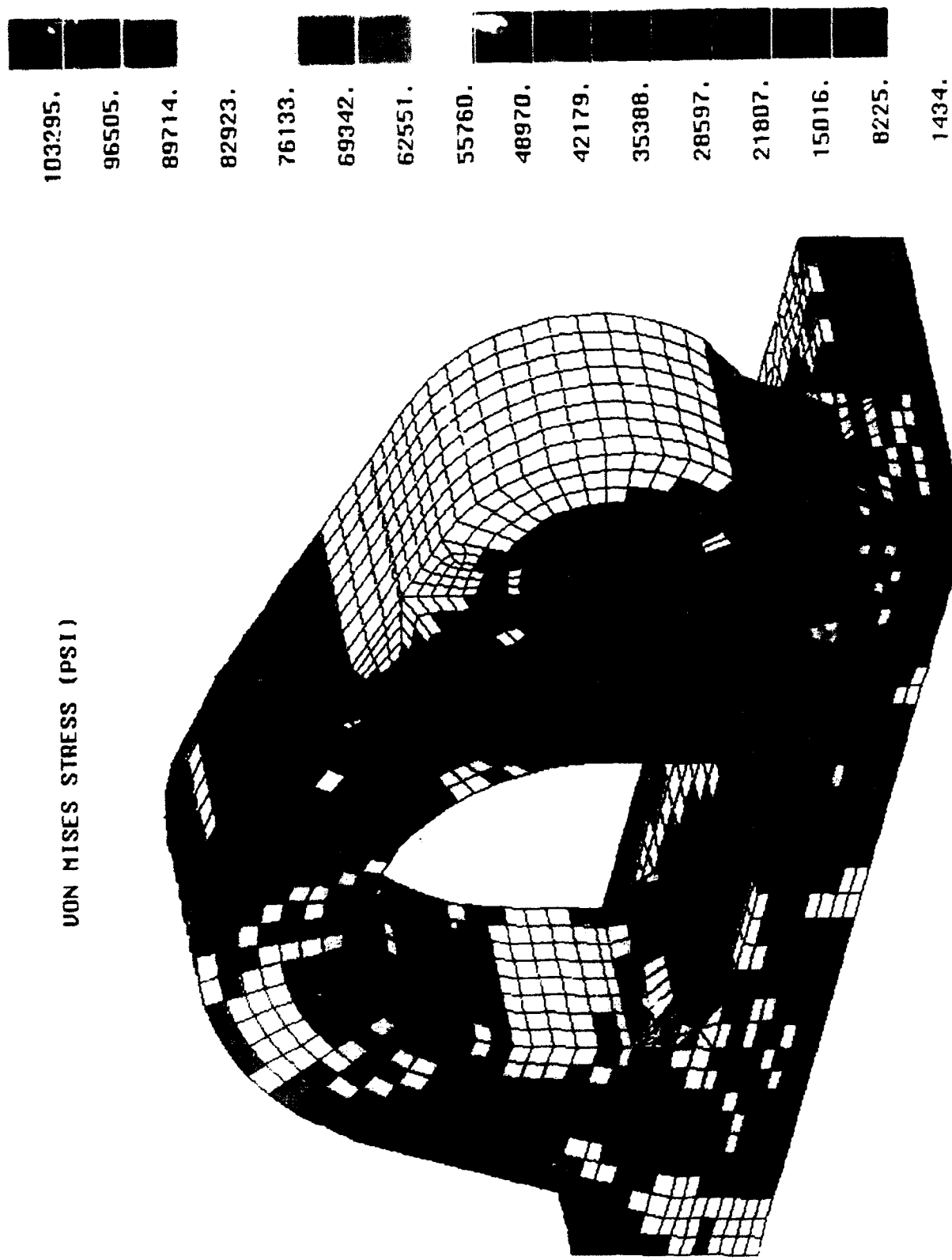


Fig. 5-17 Modified design one: Von Mises stresses at 3.45 times design load without spreader bar

File Name	Yield Strength (psi)	Ultimate Strength (psi)	Load Factor	Von Mises Stress (psi)	Location
Modtwo1	95,000	115,000	2.3	89,996	in RHA
Modtwo1	90,000	110,000	2.3	72,190	in weld
Modtwo2	95,000	115,000	3.45	115,000	in RHA
Modtwo2	90,000	110,000	3.45	92,291	in weld

TABLE 5-7. Results for Modified Design Two

VON MISES STRESS (PSI)



Fig. 5-18 Modified design two: Von Mises stresses at 2.3 times design load without spreader bar

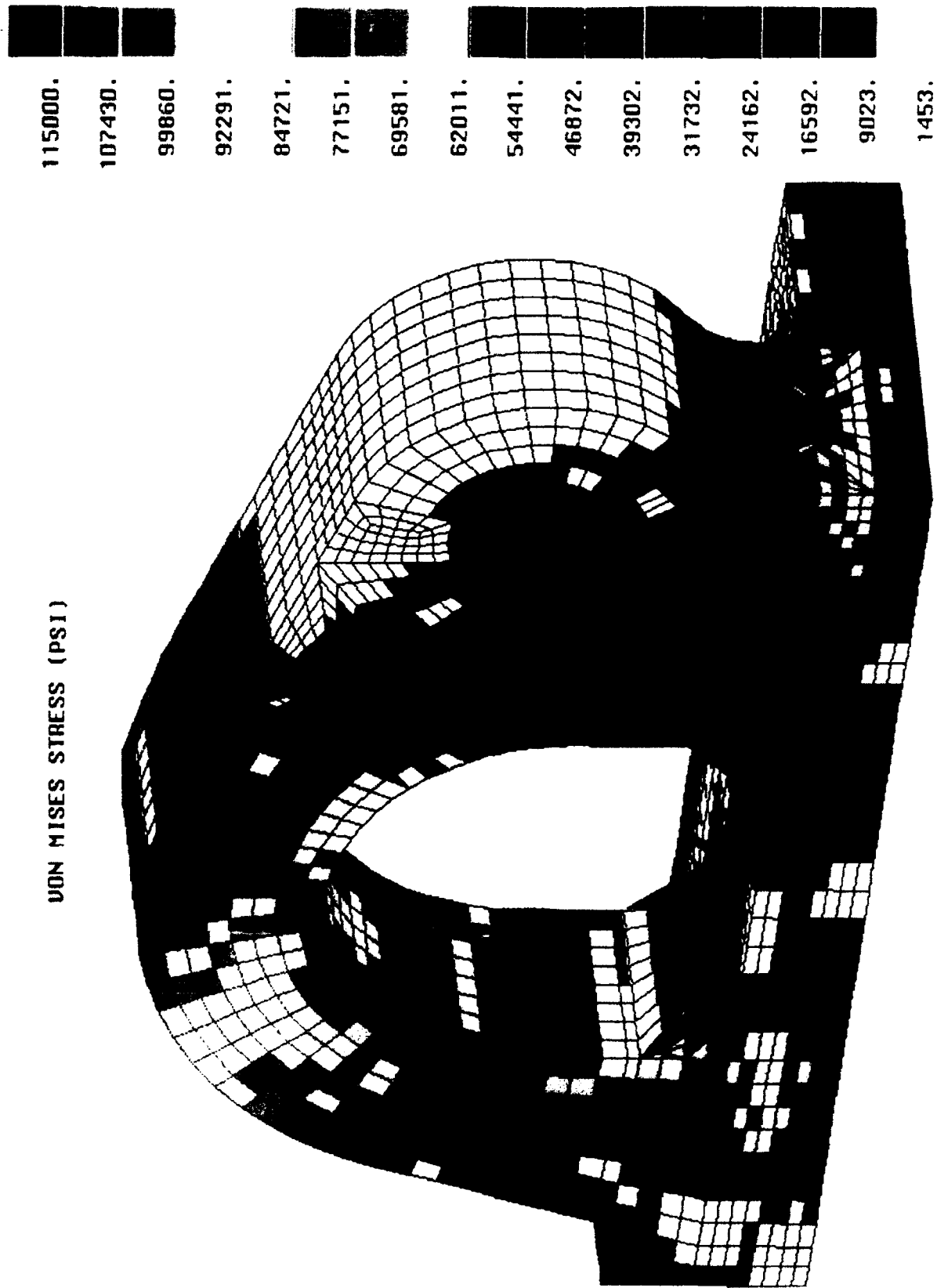


Fig. 5-19 Modified design two: Von Mises stresses at 3.45 times design load without spreader bar

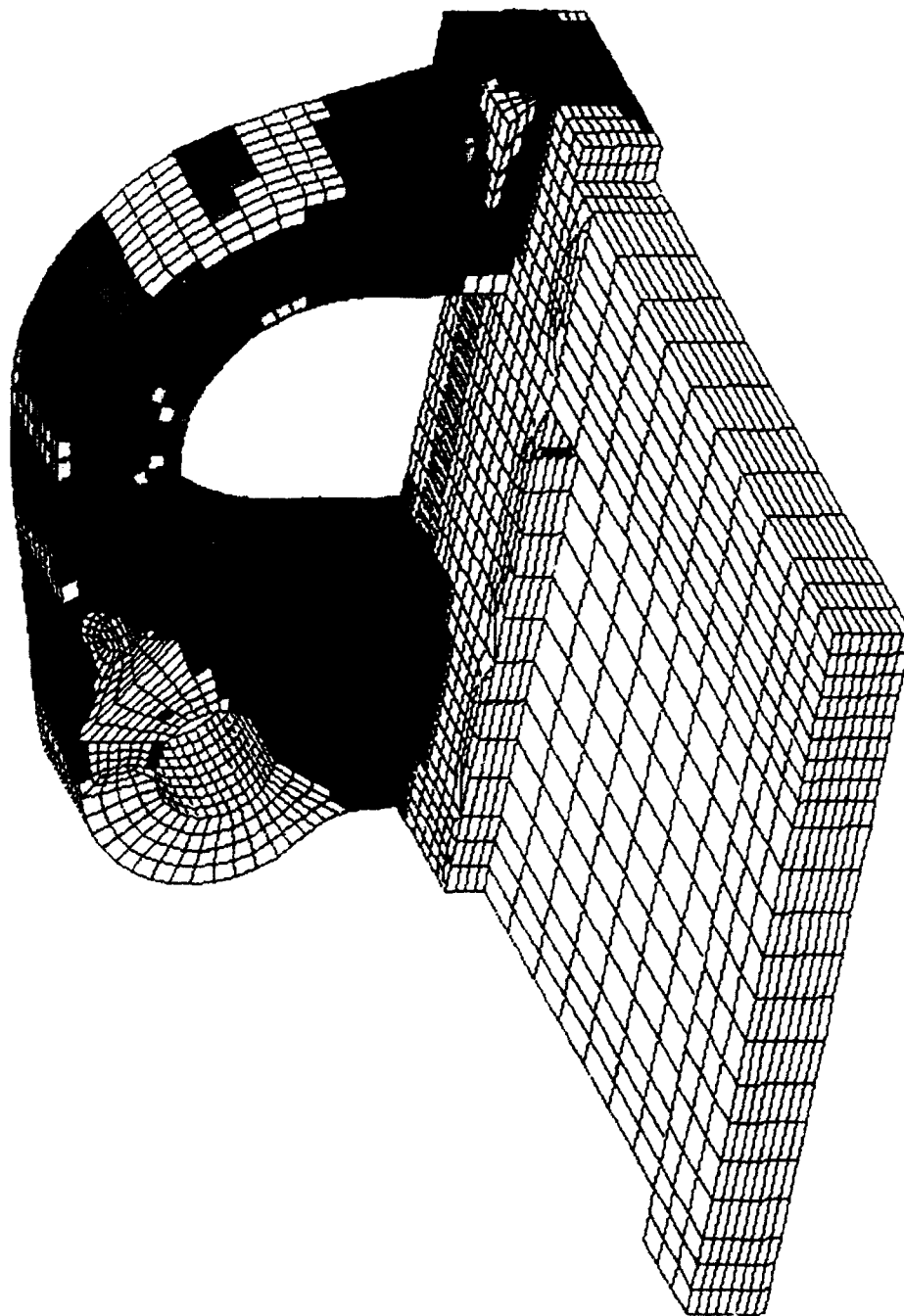
6.0. REFERENCES

1. O.C. Zienkiewicz and R.L. Taylor, THE FINITE ELEMENT METHOD, Vol. 1 and Vol.2, 4th Edition, McGraw-Hill Book Company, 1989.
2. Barna Szabo and Ivo Babuska, FINITE ELEMENT ANALYSIS, John Wiley & Sons, Inc., 1991
3. ABAQUS, Hibbitt, Karlson & Sorensen, Inc., 100 Medway Street, Providence, RI 02906.
4. PATRAN, PDA Engineering, 2975 Redhill Avenue, Costa Mesa, CA 92626

APPENDIX A

**ADDITIONAL STRESS PLOTS FOR THE
EXISTING FRONT LIFTING EYE CONFIGURATION**

VON MISES STRESS (PSI)



Inboard side of right front lifting eye.
Existing configuration.
With spreader bar, subjected to 2.3 times load.



79507.
74209.
68912.
63614.
58317.
53020.
47722.
42425.
37127.
31830.
26532.
21235.
15937.
10640.
5342.
45.0



97082.

90615.

84147.

77679.

71212.

64744.

58276.

51809.

45341.

38874.

32406.

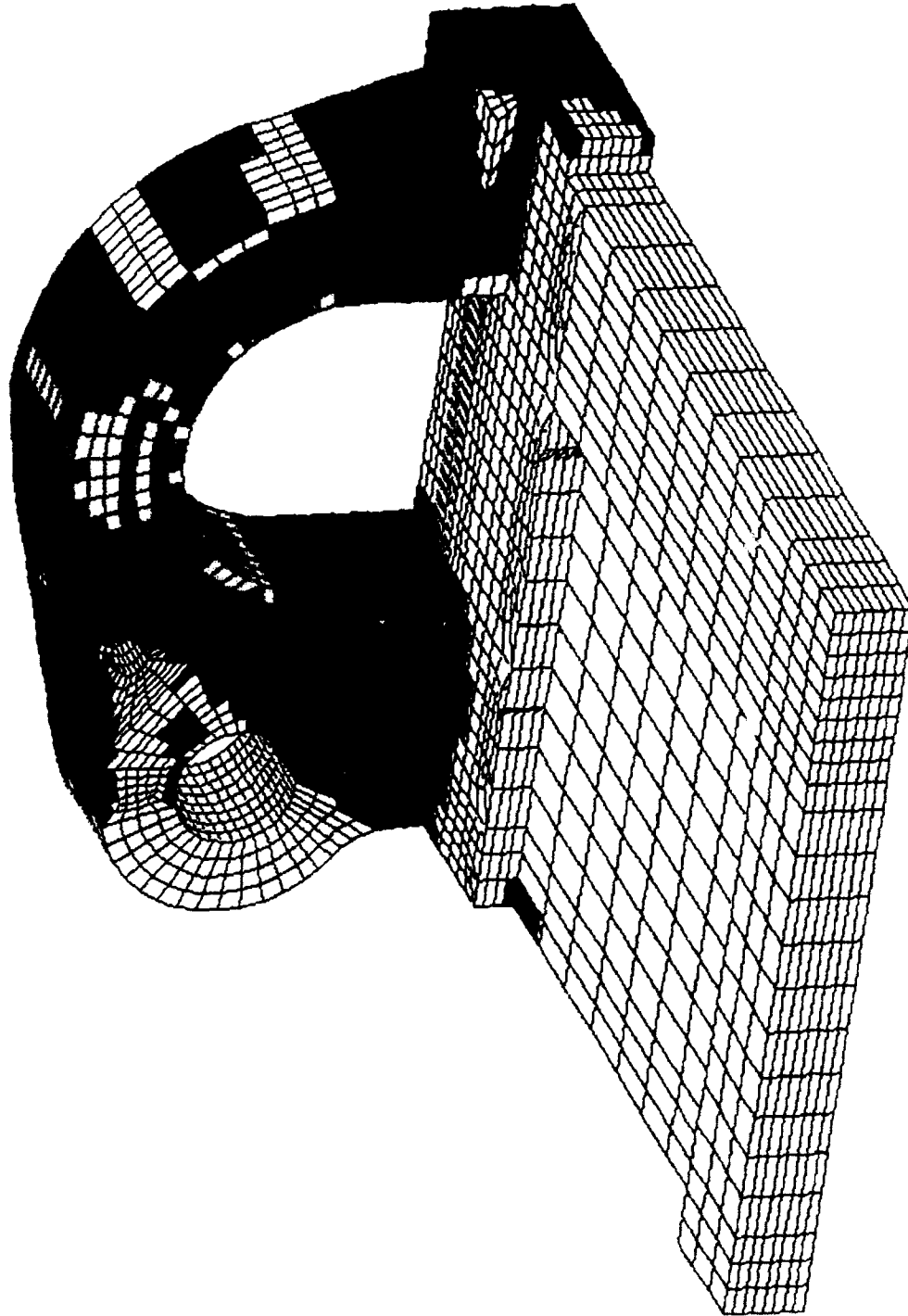
25938.

19471.

13003.

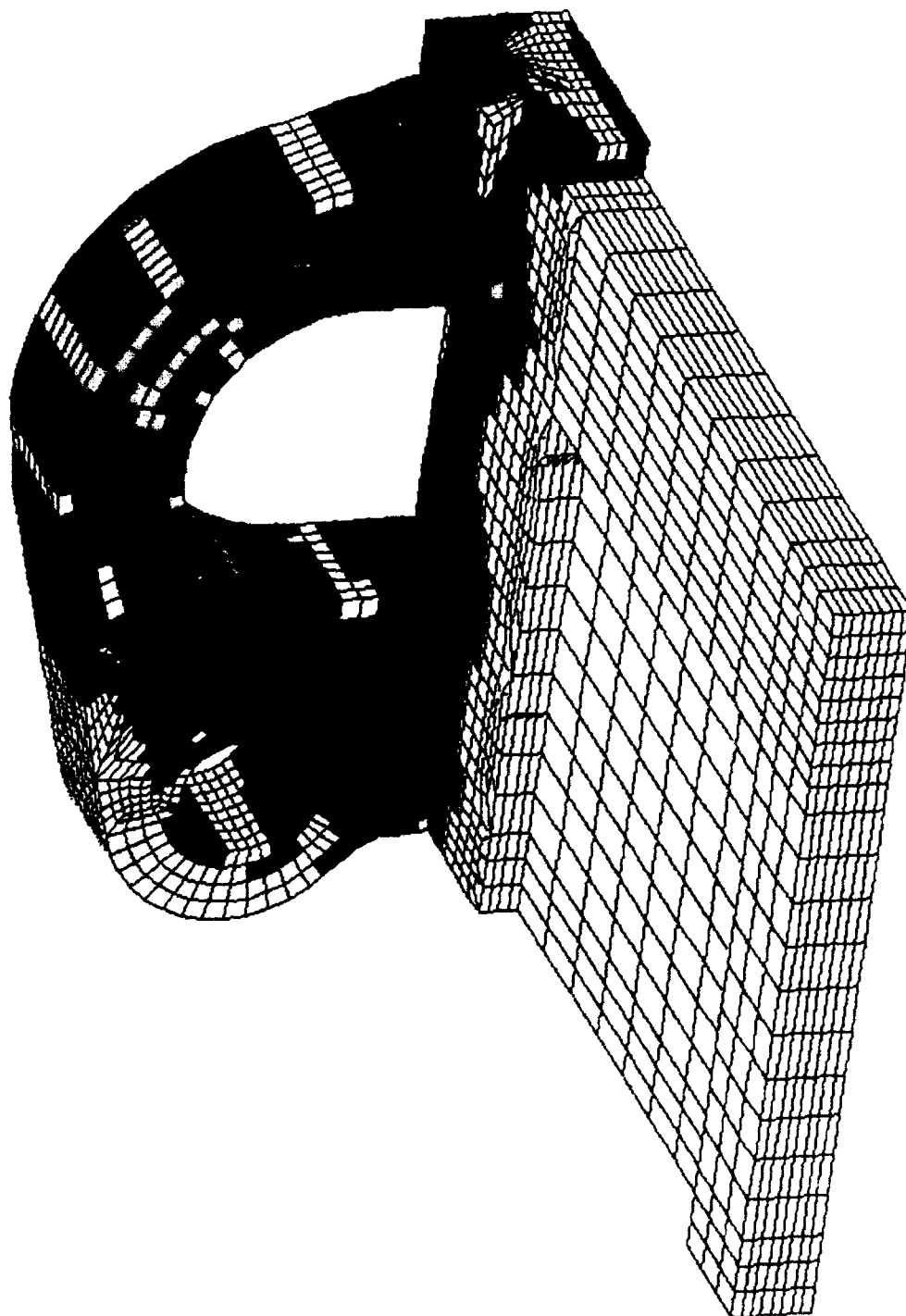
6535.

67.7



Inboard side of right front lifting eye.
Existing configuration.
With spreader bar, subjected to 3.45 times load.

VON MISES STRESS (PSI)



Inboard side of right front lifting eye.
Existing configuration.
No spreader bar, subjected to 2.3 times load.

98856.	79092.	72505.	65917.	59329.	52741.	46153.	39565.	32977.	26389.	19801.	13213.	6625.
--------	--------	--------	--------	--------	--------	--------	--------	--------	--------	--------	--------	-------

37.4



96307.

89890.

83473.



77057.

70640.

64223.

57807.



51390.

44973.

38557.

32140.

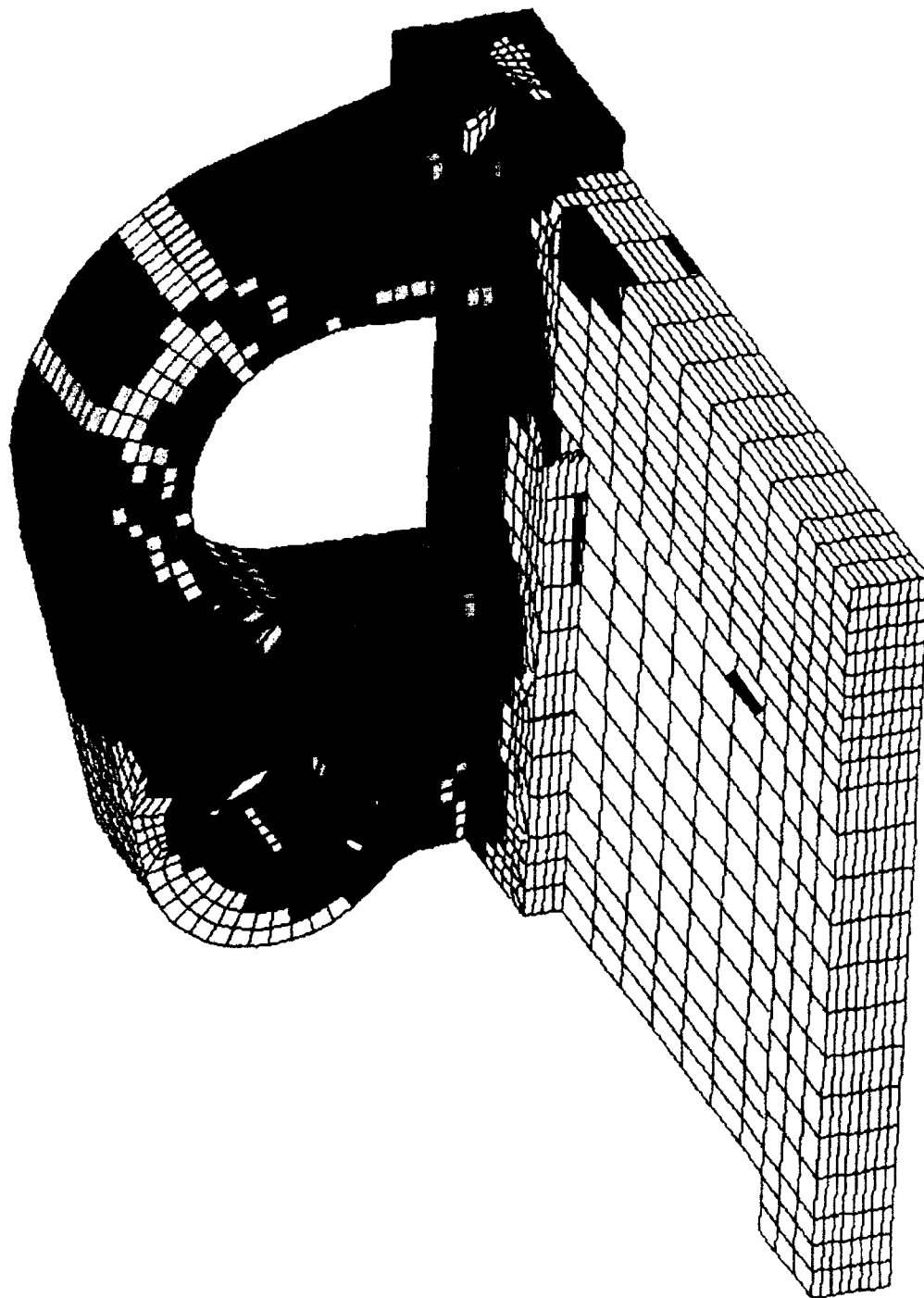
25723.

19307.

12890.

6473.

56.8

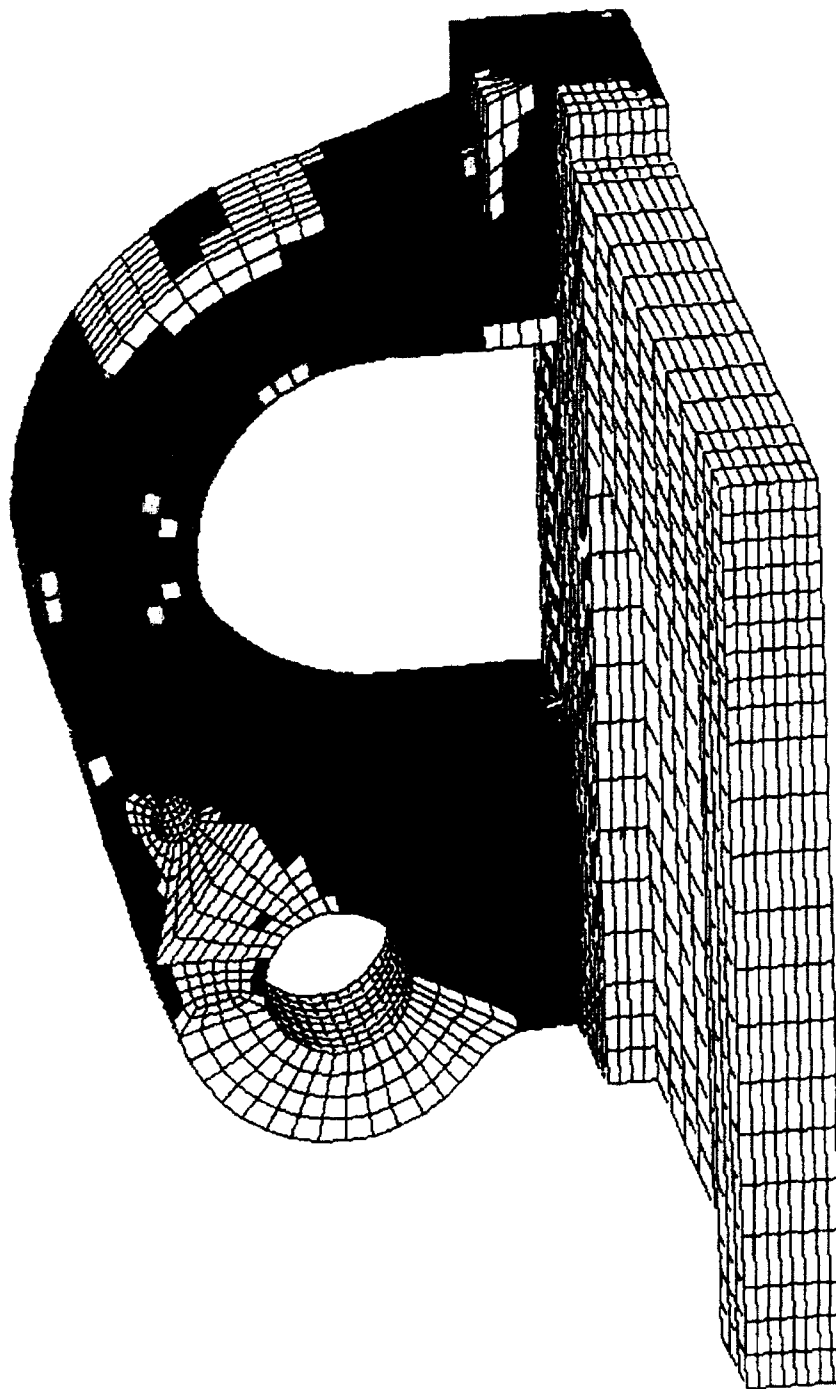


Inboard side of right front lifting eye.
Existing configuration.
No spreader bar, subjected to 3.45 times load.

APPENDIX B

**ADDITIONAL STRESS PLOTS FOR THE
FULL-PENETRATION WELD CONFIGURATION**

VON MISES STRESS (PSI)



Inboard side of right front lifting eye.
Full-penetration weld configuration.
with spreader bar, subjected to 2.3 times load.

79505.

74208.

68911.

63613.

58316.

53018.

47721.

42424.

37126.

31829.

26532.

21234.

15937.

10640.

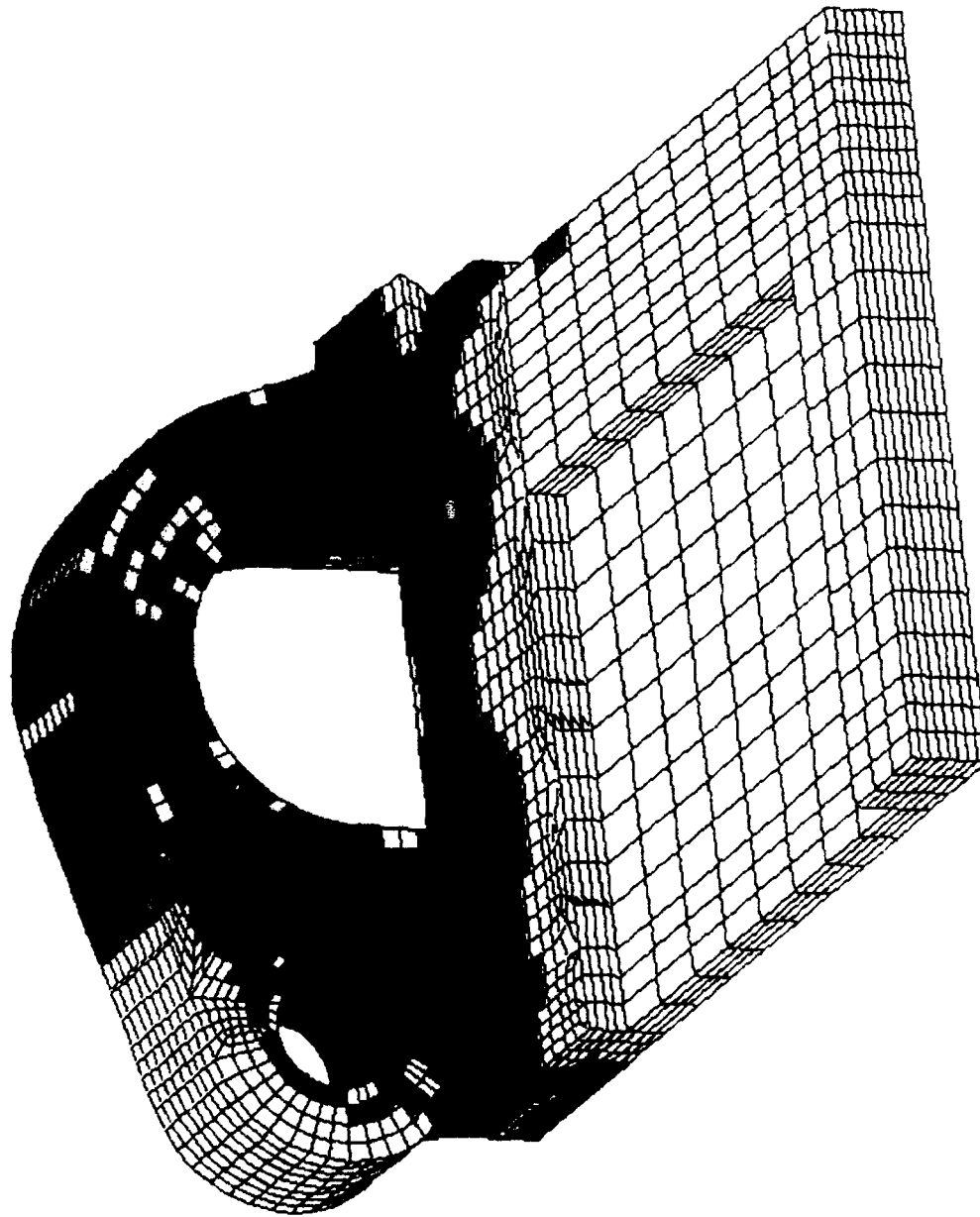
5342.

45.0

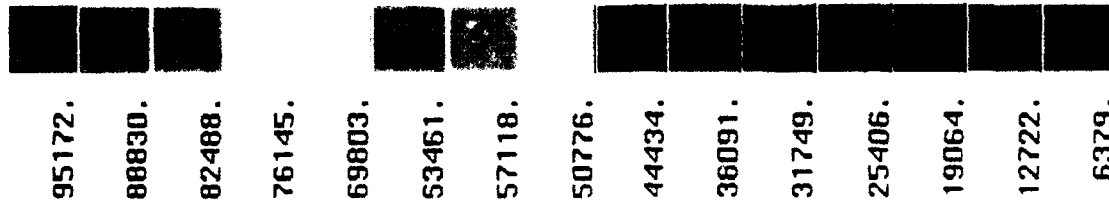
A 3D wireframe model of a mechanical part, possibly a bracket or support structure. The model is composed of a grid of lines forming a mesh. It features a curved section on the left and a vertical section on the right. The curved section has a semi-circular cutout. The vertical section has a rectangular cutout. The model is shown from a perspective view, highlighting its three-dimensional structure.

93857.	87604.	81352.	75099.	68846.	62594.	56341.	50089.	43836.	37583.	31331.	25078.	18826.	12573.	6320.
--------	--------	--------	--------	--------	--------	--------	--------	--------	--------	--------	--------	--------	--------	-------

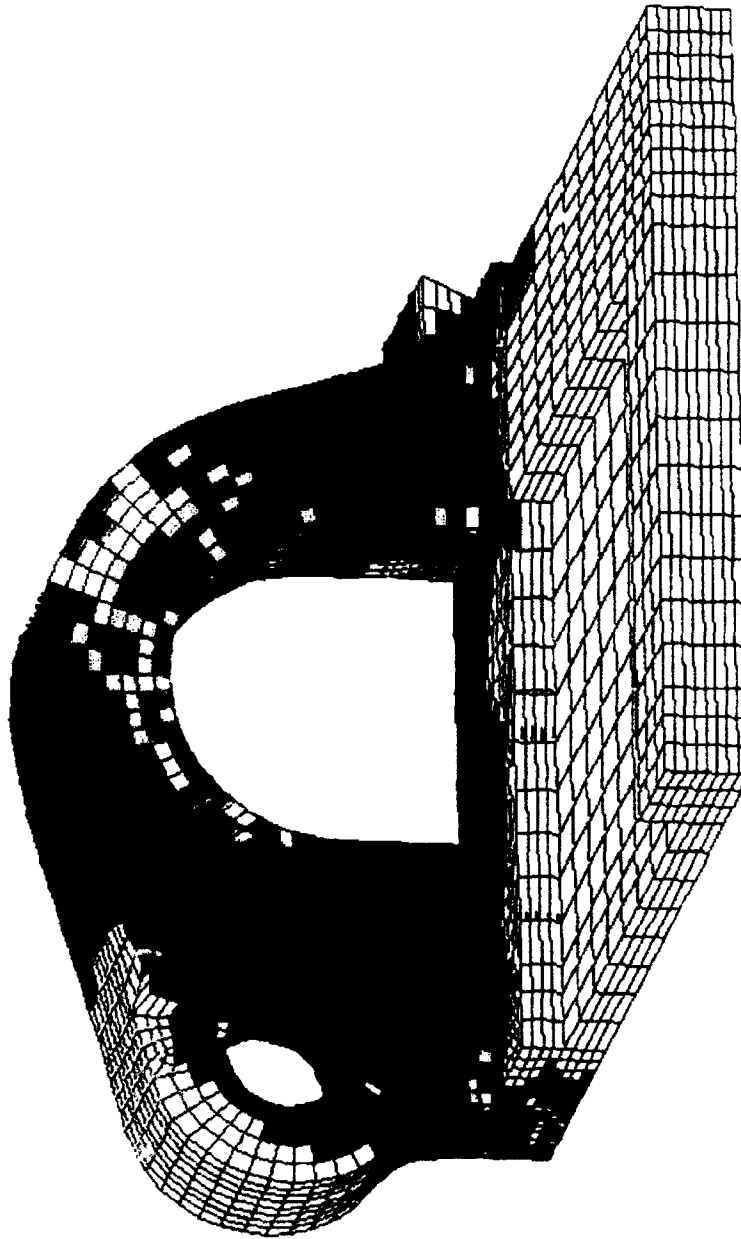
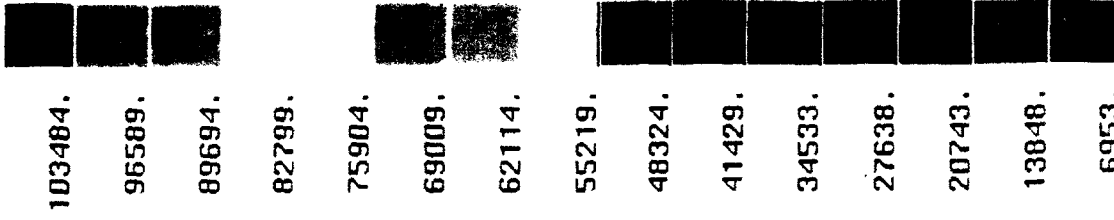
VON MISES STRESS (PSI)



Inboard side of right front lifting eye.
Full-penetration weld configuration.
No spreader bar, subjected to 2.3 times load.



VON MISES STRESS (PSI)



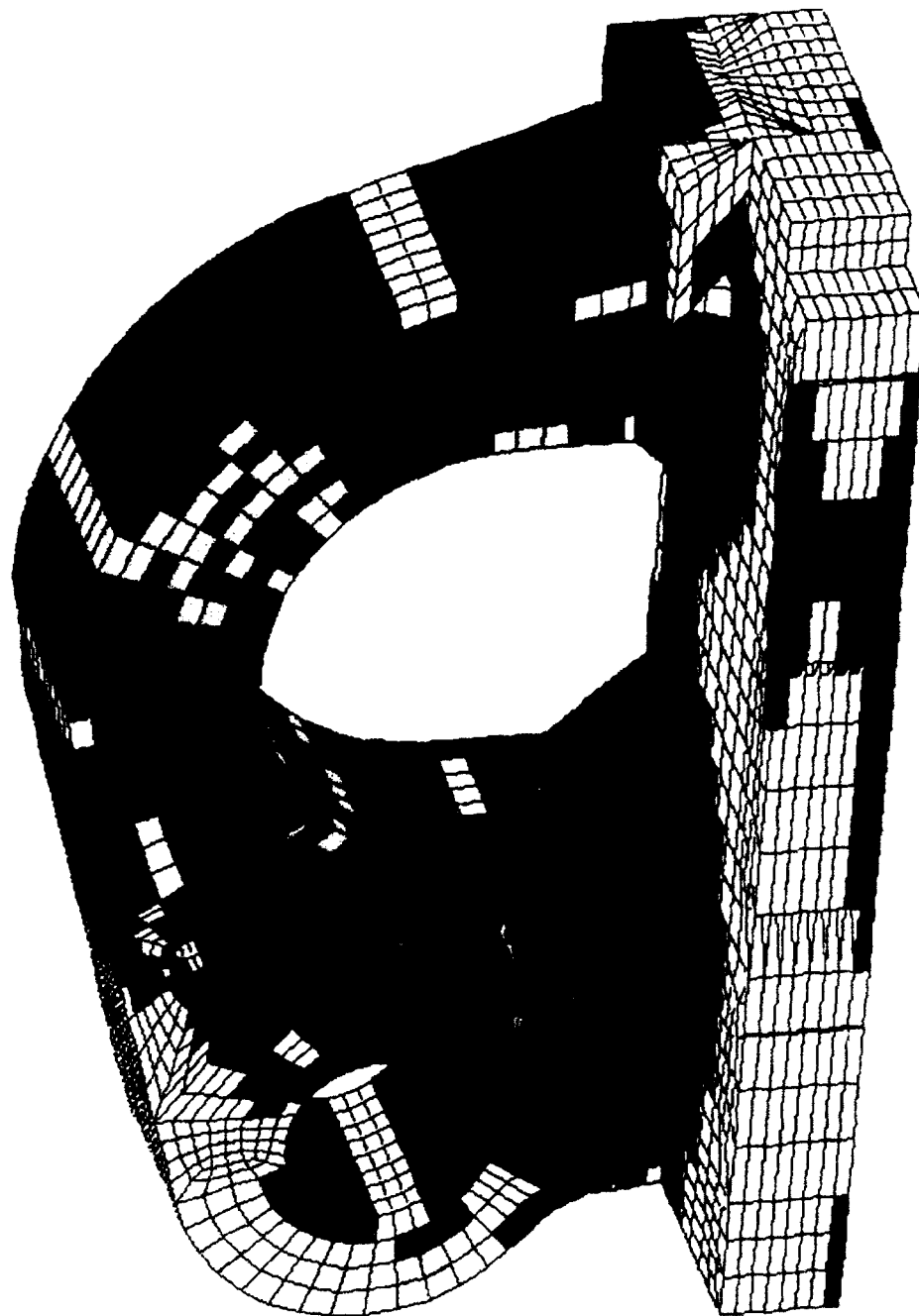
Inboard side of right front lifting eye.
Full-penetration weld configuration.
No spreader bar, subjected to 3.45 times load.

58.0

APPENDIX C

**ADDITIONAL STRESS PLOTS FOR THE
MODIFIED DESIGN ONE CONFIGURATION**

VON MISES STRESS (PSI)



Inboard side of right front lifting eye.
 Modified Design One configuration (Note additional welds).
 No spreader bar, subjected to 2.3 times load.



90935.

84936.

78936.

72937.

66938.

60938.

54939.

48939.

42940.

36941.

30941.

24942.

18943.

12943.

6944.

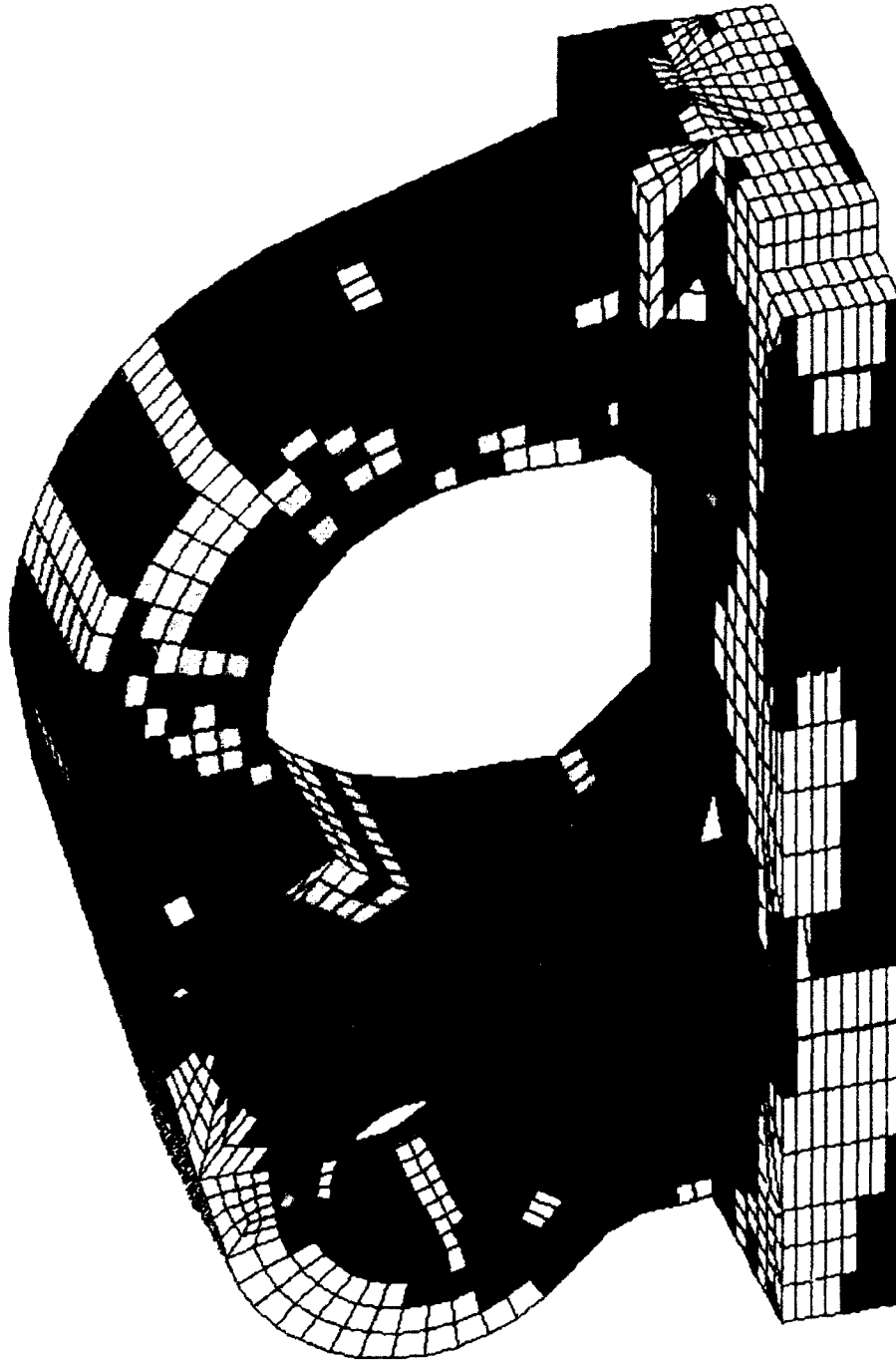
944.



VON MISES STRESS (PSI)



103295.
96505.
89714.
82923.
76133.
69342.
62551.
55760.
48970.
42179.
35388.
28597.
21807.
15016.
8225.
1434.

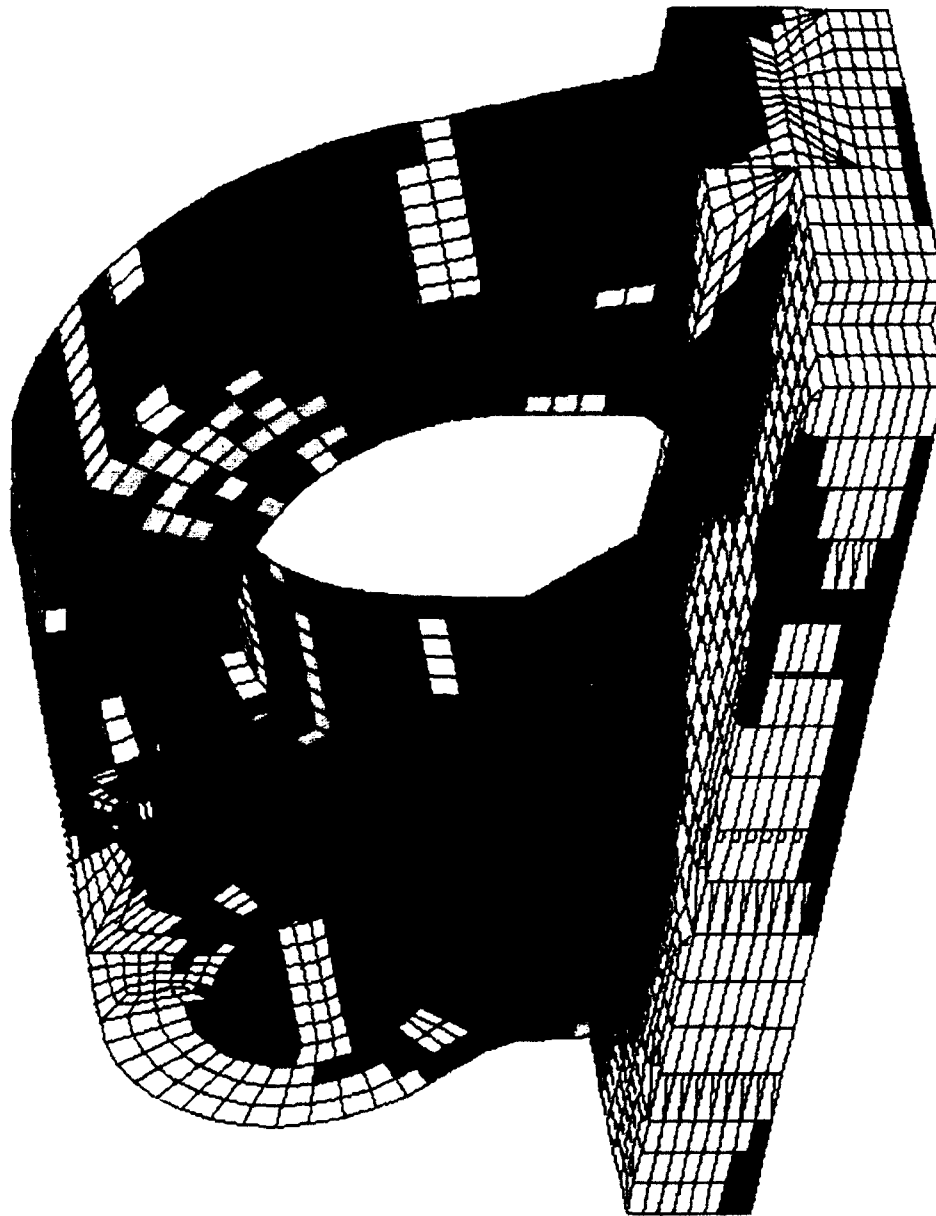


Inboard side of right front lifting eye.
Modified Design One configuration (Note additional welds).
No spreader bar, subjected to 3.45 times load.

APPENDIX D

**ADDITIONAL STRESS PLOTS FOR THE
MODIFIED DESIGN TWO CONFIGURATION**

UON MISES STRESS (PSI)



Inboard side of right front lifting eye.
Modified Design Two configuration (Note additional welds).
No spreader bar, subjected to 2.3 times load.

89996.	84061.	78126.	72190.	66255.	60320.	54384.	48449.	42513.	36578.	30643.	24707.	18772.	12837.	6901.	966.
--------	--------	--------	--------	--------	--------	--------	--------	--------	--------	--------	--------	--------	--------	-------	------

VON MISES STRESS (PSI)



115000.

107430.

99860.

92291.

84721.

77151.

69581.



62011.

54441.

46872.

39302.

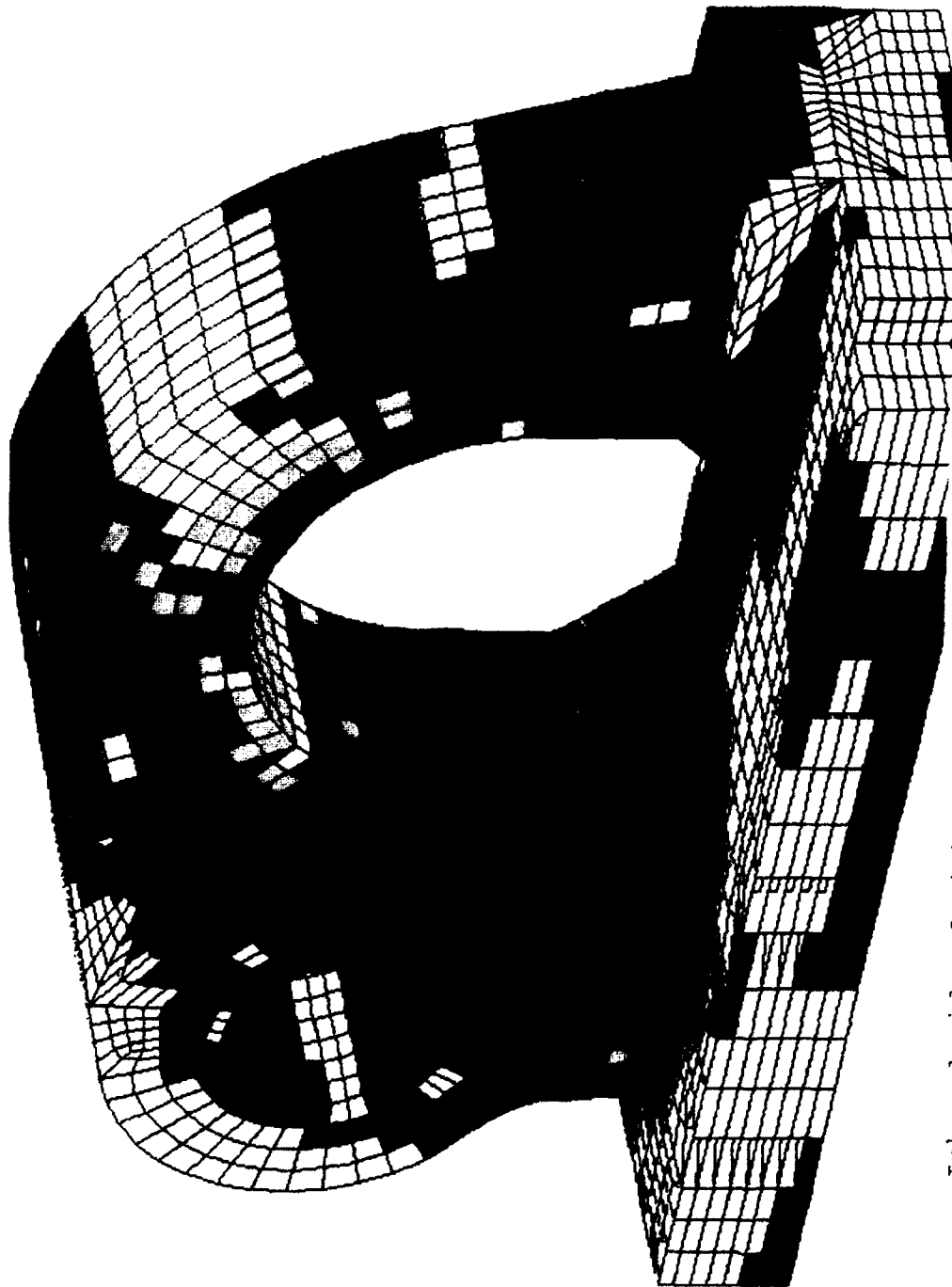
31732.

24162.

16592.

9023.

1453.



Inboard side of right front lifting eye.
Modified Design Two configuration (Note additional welds).
No spreader bar, subjected to 3.45 times load.

DISTRIBUTION LIST

	Copies
Commander Defense Technical Information Center Building 5, Cameron Station ATTN: DDAC Alexandria, VA 22304-9990	2
Manager Defense Logistics Studies Information Exchange ATTN: AMXMC-D Fort Lee, VA 23801-6044	2
Commander U.S. Army Tank-Automotive Command ATTN: ASQNC-TAC-DIT (Technical Library) Warren, MI 48397-5000	2
Commander U.S. Army Tank-Automotive Command ATTN: AMSTA-CF (Dr. Oscar) Warren, MI 48397-5000	1
Director U.S. Army Material Systems Analysis Activity ATTN: AMXSY-MP (Mr. Cohen) Aberdeen Proving Grounds, MD 21005-5071	1
Director Military Traffic Management Command Transportation Engineering Agency ATTN: MTTE-TRV (Melvin Sutton) Newport News, VA 23606-2574	1
Commander U.S. Army Tank-Automotive Command ATTN: PM Abrams (Mr. Rzyzi) Warren, MI 48397-5000	1
Commander U.S. Army Tank-Automotive Command ATTN: PM Abrams (Mr. Vander Waerden) Warren, MI 48397-5000	1
Commander U.S. Army Tank-Automotive Command ATTN: PM Abrams (Mr. Kim) Warren, MI 48397-5000	10

Commander U.S. Army Tank-Automotive Command ATTN: PM Abrams (Mr. Harju) Warren, MI 48397-5000	1
Commander U.S. Army Tank-Automotive Command ATTN: AMSTA-RYC (Mr. Lambrecht) Warren, MI 48397-5000	10
Commander U.S. Army Tank-Automotive Command ATTN: AMSTA-JSK (Mr. Rostam-Abadi) Warren, MI 48397-5000	5
Army High Performance Computing Research Center ATTN: Mr. Muzio 1100 Washington Ave. South Minneapolis, MN 55415	1
General Dynamics Land Systems Mail Zone 439-01-07 ATTN: Mr. Said Samaan Warren, MI 48090-2094	3
Computer Sciences Corporation ATTN: Mr. Pinkerton Mail Code 321 3160 Fairview Park Dr. Falls Church, VA 22042	1